EARLE,

FOR YOU.

0304-3800/86/$03.50

PRINTED IN THE NETHERLANDS

Ecological Modelling, 34 (1986) 1–59
Elsevier Science Publishers B.V., Amsterdam – Printed in The Netherlands

A COMPUTER SIMULATION MODEL OF THE SOLAR–ALGAE POND ECOSYSTEM

JOHN R. WOLFE, RONALD D. ZWEIG and DAVID G. ENGSTROM
The New Alchemy Institute, 237 Hatchville Road, East Falmouth, MA 02536 (U.S.A.)

(Accepted 2 July 1985)

ABSTRACT

Wolfe, J.R., Zweig, R.D. and Engstrom, D.G., 1986. A computer simulation model of the solar–algae pond ecosystem. *Ecol. Modelling*, 34: 1–59.

A comprehensive analysis of the 2300-l solar–algae pond (translucent fiberglass silos 1.5 m in diameter and height) used for the culture of the blue tilapia, *Oreochromis aureus*, was conducted to determine the impact of pond management upon water quality and rate of fish growth. Studies were done within a variety of seasonal conditions and management regimes over a 5-year period at the New Alchemy Institute.

The findings have been mathematically represented through System Dynamics modelling. The model, coded in DYNAMO, ties together all elements and causal relationships determined significant from the experimentation. The mathematical simulations successfully reproduce with good detail the aquatic ecosystem maturation of three experimental runs over a 100-day period. The subsections within the model include fish, algae, exogenous variables (feeding, fish stocking density, sunlight, water exchange, aeration), suspended organic particles, ammonia, nitrite, nitrate, oxygen, carbon dioxide, alkalinity and five groups of bacteria. The model shows which areas of the system are metastable and rather unpredictable, which regimes are stable and resist outside influences, and which parameters yield entry points into more effectively managing and optimizing the ecosystem's productivity. It further reveals specific areas where more basic research is required.

INTRODUCTION

From 1975 through 1981, the New Alchemy Institute researched and perfected a high density fish culture system housed in highly translucent 2300-l cylinders termed 'solar-algae ponds' (Zweig, 1977) (see Fig. 1). The blue tilapia, *Oreochromis aureus*, grown in the solar-algae ponds have a

This project was supported in part by scientific research grants from the National Science Foundation, Nos. OPA7716790 and ISP-8016577

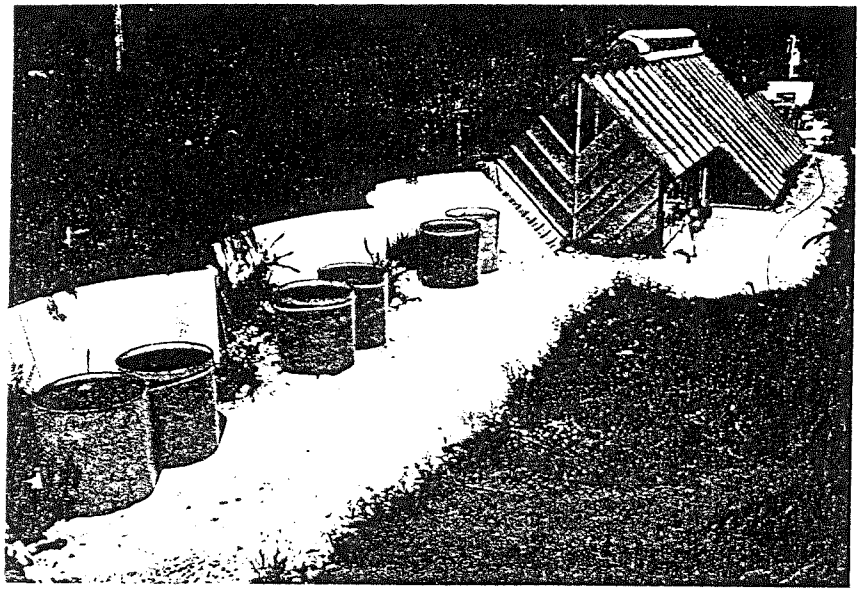

Fig. 1. Six solar-algae ponds in the east reflective courtyard adjacent to the Cape Cod Ark bioshelter. The acrylic tops were removed during the experimentation (photo by Earle Barnhart).

profound dependence on the microbial ecosystem through which they swim (Zweig et al., 1981). The algae and bacteria not only feed the fish, they cause the chemical transformations that will either protect or harm the fish. The aquatic ecosystem that resides in the 1.5 m in height and diameter, translucent fiberglass-reinforced polyester (FRP) silos is unique: solar fluxes are four to five times higher than a typical pond of equal depth (Wolfe et al., 1980), the fish are omnivorous filter feeders native to Africa and the Middle East living at densities two to three orders of magnitude greater than natural ponds, the organic loading in the form of fish feed is correspondingly unnatural, and the photosynthetic, bacterial and chemical activity is exceptionally rapid. A study of fish culture in solar-algae ponds demands a broad study of the entire ecosystem. A rigorous inquiry into the nature of this ecosystem demands a mathematical model that ties together all the quantitative observations of the components into an interacting whole.

Ecosystems have characteristics that set baseline criteria for mathematical modelling methodology. They include:

(1) feedback, interconnectedness;

(2) nonlinearities; relationships described by plateaus, breakpoints and sigmoidal curves;

(3) delays and accumulations; and

(4) non-equilibrium or transient dynamics.

To meet these criteria, the ecosystem model we have developed numerically simulates nonlinear differential equations involving complex feedback (for a theoretical justification of this approach, see Forrester, 1969; Young et al. 1970; May, 1975, 1976; Jørgensen et al., 1978).

An explicit modelling methodology, System Dynamics, can be used to accomplish the task well. Forrester developed the discipline at the Massachusetts Institute of Technology's Sloan School of Management in the late 1950's to analyze complex industrial management problems, and later socio-economic questions (Forrester, 1968a, 1968b, 1973; Meadows et al., 1972; Goodman, 1974; Meadows et al., 1974). The conventions of the methodology emphasize important structural distinctions, such as levels versus rates, endogenous versus exogenous variables, and feedback versus one-way causality. Behrens et al. (1975) and Pieri and Converse (1974) argue that System Dynamics holds great prmise for aquatic ecosystem modelling. A computer language called DYNAMO (Koch, 1975; Pugh, 1977; Shaffer, 1978), or its offshoot NDTRAN (Davisson and Uhran, 1977), greatly facilitate System Dynamics modelling. The model described herein, coded in DYNAMO, ties together all elements and causal relationships currently thought significant by the solar aquaculture research staff, and successfully reproduces in good detail the maturation of several solar-algae ponds closely observed over a 100-day period. Those results have given us the confidence to simulate untested solar-algae pond fish culture situations, and draw some ecosystem management principles, policies and rules-of-thumb from the model.

The DYNAMO compiler simulates complex systems by stepping through time in very small increments. This increment is called the simulation's computation interval, or 'DT'. The compiler first assembles all the initial data. This start-up information includes the beginning values of the program's state variables or LEVELS (e.g., fish biomass), along with any CONSTANTS (e.g. the nitrogen content of fish feed) and externally defined ('exogenous') AUXILIARY variables (e.g. solar radiation). From this information the DYNAMO compiler computes all intermediate AUXILIARY variables. These values in turn determine the RATE values. The RATES, multiplie over the time increment DT, increase or decrease the LEVELS and give them new values for the next point in time. External variables are updated, and the process continues: levels determining auxiliaries that determine rates that in turn define new levels at the next point in time. This interactional 'bootstrapping' through time simulates the causal linkage between all components of the system, and determines the path of all variables through time.

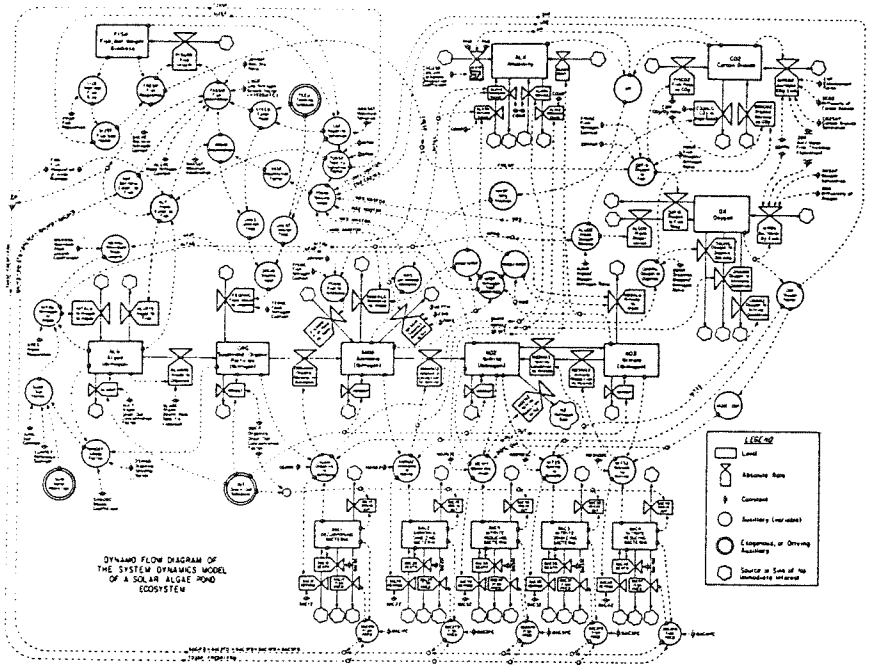

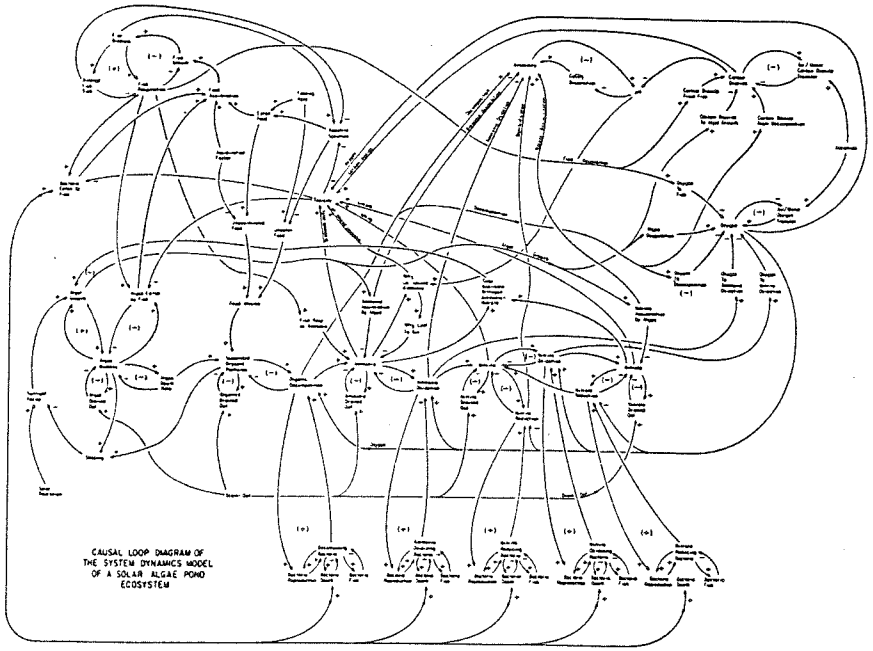

Fig. 2. Dynamo flow diagram of the system dynamics model of a solar-algae pond ecosystem, and the casual loop diagram.

The model described hereafter has a causal structure illustrated in Fig. 2. This is the model's DYNAMO Flow Diagram. At a glance the reader can note all the levels in the model, indicated by the rectangular box symbols. The complex interwoven relationships connecting these levels require closer examination. Physical flows are diagrammed with solid lines, while causal relationships are represented by dotted lines. Rates, shaped like valves or milkcans, drain or replenish the levels. The circular auxiliaries tie levels back to rates, either directly, or indirectly by involving several auxiliaries in a chain. The exogenous variables are indicated by double circles; important controllable constants are marked by double bars. Figure 2 details every causal relationship currently in the model, giving the reader a map for guidance and perspective while proceeding through the following description of the model's sectors.

FISH SECTOR

The critical aspects of fish growth that we have modelled include the following:

(1) The net growth or decline in fish biomass is determined by the difference between food assimilation and respiration.

(2) Food assimilation depends on the amount of food eaten, and on the assimilation efficiency.

(3) Fish respiration is a function of fish biomass and average fish size.

(4) Water chemistry, represented by a toxicity index, affects the assimilation efficiency.

(5) The amount of food eaten equals the amount of food available, unless the available food exceeds an appetite satiation limit.

(6) The food available falls into several categories: introduced feed, filtered out algae and bacteria-laden organic particles. Filtering rates depend on total fish respiration and the concentrations of algae and bacteria.

(7) Fish respiration and the toxicity index determine the appetite satiation limit.

Figure 3 represents these relationships with a causal loop diagram. Walking through loop 1 can bring clarity. Increased FISH BIOMASS increases FISH SIZE. The greater the FISH SIZE, the lower the respiration per unit of body weight. If the biomass is held constant, increasing fish size

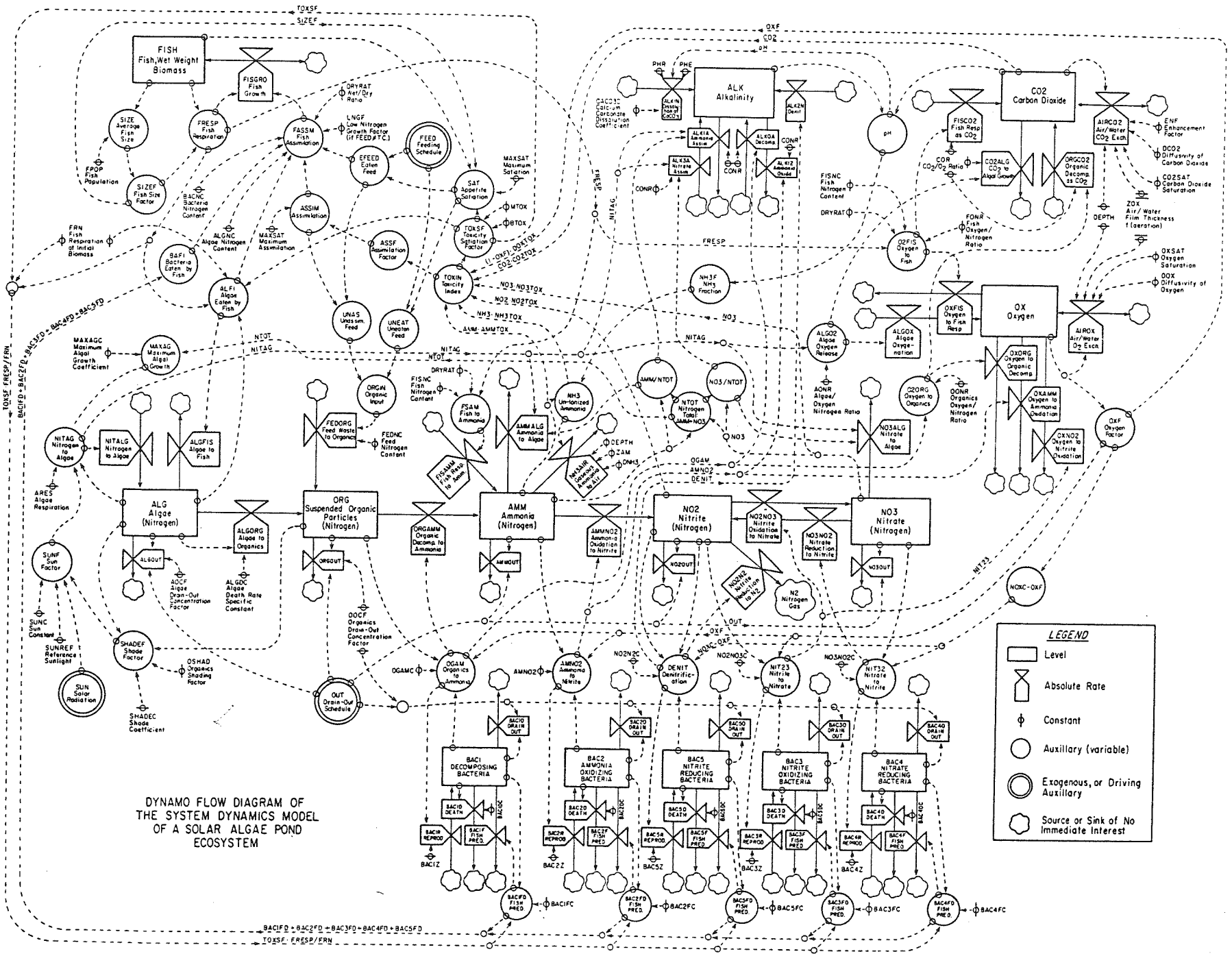

DYNAMO FLOW DIAGRAM OF THE SYSTEM DYNAMICS MODEL OF A SOLAR ALGAE POND ECOSYSTEM

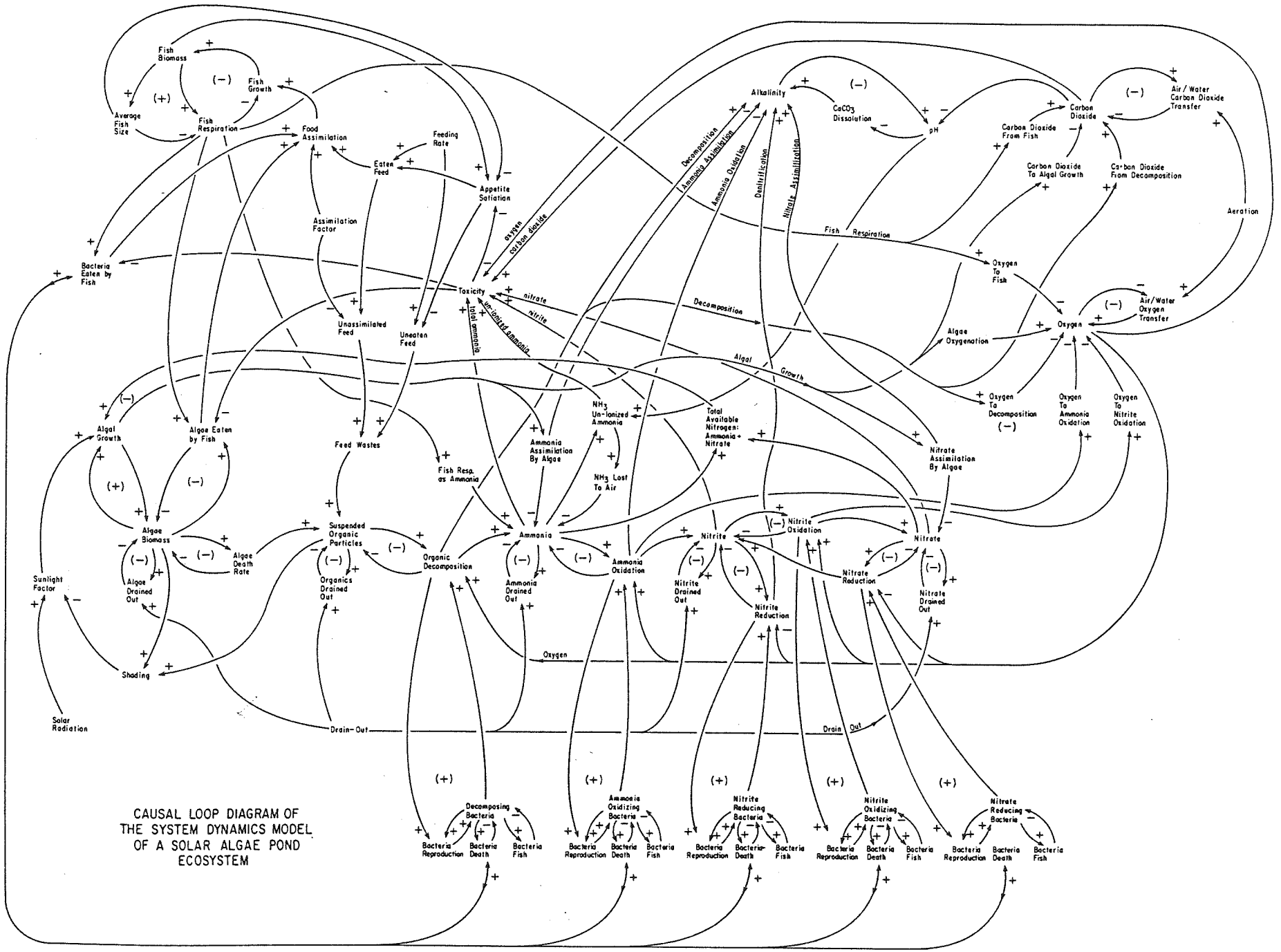

CAUSAL LOOP DIAGRAM OF THE SYSTEM DYNAMICS MODEL OF A SOLAR ALGAE POND ECOSYSTEM

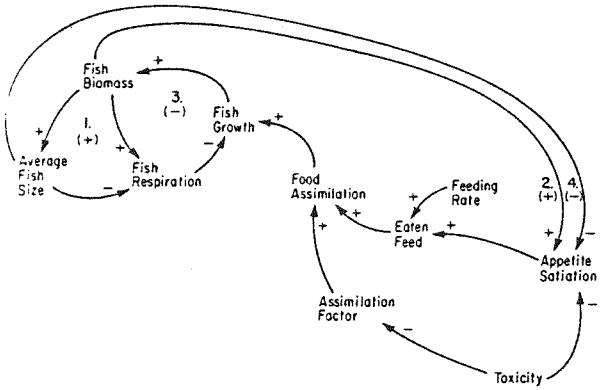

Fig. 3. Causal loop diagram of simplified fish growth sector.

lowers total respiration. Lowered FISH RESPIRATION increases FISH GROWTH, which in turn increases FISH BIOMASS. The two negative causal connections lead to positive feedback: an increase in FISH BIOMASS cascades through the loop and leads to even more fish biomass.

Positive loop 1 does not lead to exponential fish growth because it is heavily moderated by the native feedback of loop 3: increased FISH BIOMASS creates greater FISH RESPIRATION, which in turn causes less FISH GROWTH and thus less FISH BIOMASS.

Loops 2 and 4 involve a satiation feeding limit. Because respiration per body weight decreases as fish size increases, satiation per body weight also falls as fish size climbs. If feeding exceeds the total satiation limit, the fish will only eat up to that limit. The rest of the feed will remain uneaten. The positive link between satiation and eaten food is only active when feeding rates are overly generous. Therefore loops 2 and 4 are conditional loops, depending on feeding rates exceeding appetite satiation.

This simple cuasal loop diagram adequately describes the culture of fish in cages floating in open ponds, or in fast water flow-through aquaculture. In both cases, feeding rates and fish respiration have virtually no impact on water quality. In closed aquaculture systems, however, fish respiration and feeding rates strongly affect water quality. Figure 4 incorporates the TOXICITY INDEX into a feedback loop. This amendment is a gross oversimplification of the ammonia, nitrite, oxygen, carbon dioxide, organics, algal and bacterial sectors of the comprehensive model, to be described later in this paper.

In this (albeit still oversimplified) drawing, one readily sees the classic dilemma of the closed system aquaculturist. The most easily controlled

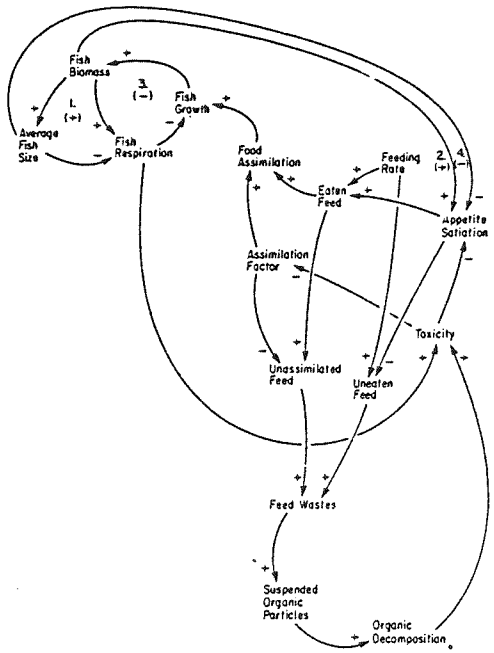

Fig. 4. Causal loop diagram of simplified fish growth sector, including feedback loops through toxicity.

variable—the feeding rate—has both profound positive and negative effects on fish growth. The feeding rate positively affects fish growth immediately through increased food ingestion and assimilation; after a delay, it also negatively affects fish growth because any unassimilated food or (in the case of overfeeding) uneaten food eventualy decomposes, increasing the toxicity index. The toxicity index decreases both the assimilation efficiency and the appetites of the fish.

Figure 4 shows all the positive and negative feedback loops that are present, but it cannot indicate which loops are dominant at any point in time or with any combination of factors. The equations of the computer model quantify the concepts and assumptions embodied in Fig. 4.

ALGAE SECTOR

The presence of algae in the solar-algae ponds has been considered by this research staff to be an intrinsic and beneficial element in solar aquaculture. This positive attitude toward phytoplankton is not shared by most other

aquaculturists. The common belief is that algae are to be avoided and should be posoned, shaded or filtered out. Their reasoning is that algae are instable and susceptible to sudden die-offs. The rapid decomposition that follows causes devastating changes in water quality.

In contrast to the prevailing fish farmaer's view toward algae, the New Alchemy staff have pointed out four ways that a thriving algae population can aid fish culture. The algae, while growing:

(1) produce oxygen through daytime photosynthesis that exceeds nighttime algal respiration;

(2) remove through assimilation highly toxic ammonia and carbon dioxide, and less toxic nitrate and phosphate;

(3) provide a diet supplement to the herbivorous tilapia that is very likely to be rich in critical vitamins and amino acids; and

(4) absorb virtually all solar radiation that penetrates the side walls of the solar algae ponds, allowing the water to act as a very efficient solar collector/heat storage unit.

A significant body of literature exists showing that in outdoor ponds fed little or no fish rations, fish growth is strongly correlated with net and gross algal photosynthesis (e.g., McConnell, 1965; Arce and Boyd, 1975; Almazan and Boyd, 1978; Yanling et al., 1981). The correlation probably stems from our third point, algae acting as a feed. Algae can be eaten directly by both herbivorous fish and zooplankton. The zooplankton in turn act as highly nutritious fish food.

However, room still exists for skepticism about the role of algae in the context of solar–algae ponds. In contrast to the outdoor ponds cited, solar–algae ponds are fed very heavily and stocked at densities two orders of magnitude greater than typical outdoor fish farm ponds. The high fish densities have a profound impact on the balance of microbial species in the solar–algae ponds (this is a widely noted phenomenon; for instance, see Brooks and Dodson, 1965). Microcrustacean zooplankton are virtually nonexistent due to enormous predation pressure, as are most algae except for green algae species small enough to reduce the likelihood of filtration by the tilapia and heavily enough armored with thick cell walls to usually survive passage through the tilapia's digestive system. Microscopic examination first performed by Deborah Goodwin in 1978, and since verified, of live algae and lysed cell walls at the beginning and end of a sacrificed tilapia's digestive tract indicate that as much as 95% of *Scenedesmus* cells may survive the passage. Pond D in the 1978 experiments (Progress Report 3, p. 32, Fig. 8b), with only fertilizer inputs and no externally introduced feeds, shows that over the long term the algae provide enough calories of food to just cover the basal metabolic needs of 2 kg of tilapia.

In addition to evidence for a reduced dietary contribution from algae, the

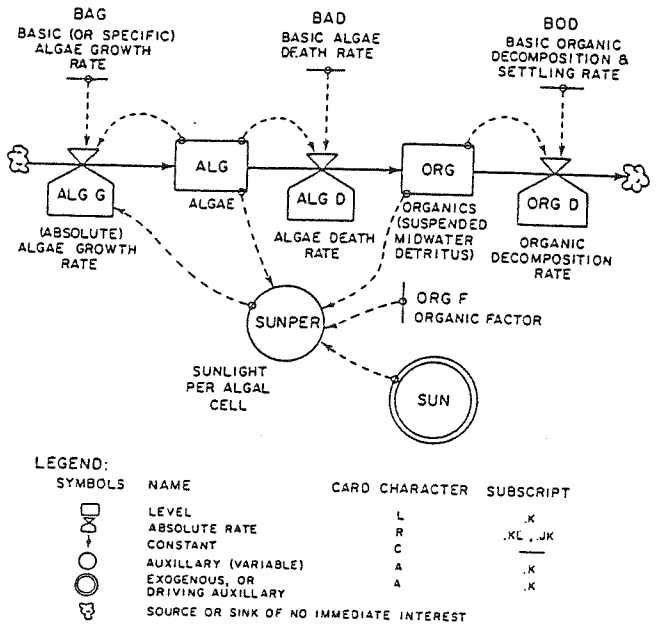

Fig. 5. DYNAMO flow diagram of algae growth model.

algae population instabilities cited by many fish farm researchers have been observed in solar-algae ponds. All the ponds in the late summer 1978 experiment exhibited remarkably similar algae growth and collapse patterns. Progress Report 4 (pp. 55–65) listed three possible explanations for the algal crash, based on the amount of light available to each algal cell. A simple DYNAMO model was then constructed that tested the three hypotheses. Figure 5 illustrates the DYNAMO flow diagram of this initial, simplified algae model. Results from the model rejected the first two hypotheses, while upholding the third. The hypotheses are:

(1) A period of sunny weather was followed by a period of cloudy weather (causes gradual random fluctuations, not a strong overshoot and collapse).

(2) The algae grew to a point where they shaded each other's incoming light (causes sigmoidal growth to a plateau).

(3) Shading occurred not only from live algal cells, but also dead algal cells still suspended in the water column (can cause overshoot and collapse).

Wolfe et al. (1981) postulate three more hypotheses:

(4) Invasion by bacteria that prey upon the algae.

(5) Generation by the algae of a metabolic toxin that suppressed further algal growth.

(6) Depletion of a critical limiting micronutrient.

Hypotheses (4)–(6) were rejected because in each of the ponds observed, radically different algal species exhibited nearly identical population growth patterns. It is highly unlikely that the mechanisms of bacterial predation, metabolic toxins (such as iron chelating agents, Murphy et al., 1976), or micronutrient deficiency would act identically on each of the three different dominant algae genuses observed. The sixth hypothesis is even unlikier because the elemental inputs are in organic form (as fish feed) that should contain all micronutrients. Because of slow water exchange, all inputted elements tend to increase over time in concentration, as demonstrated by the high and increasing concentrations of soluble inorganic nitrogen and phosphate.

The current model upholds a seventh hypothesis, based on the concept of light starvation (like hypotheses (1)–(3)), that expands hypothesis (3) to include shading from fish feed wastes:

(7) ?Shading occurs from live algal cells, dead algal cells, and most importantly, particulate fish feed wastes.

A causal loop diagram of the algae submodel, based on the seventh

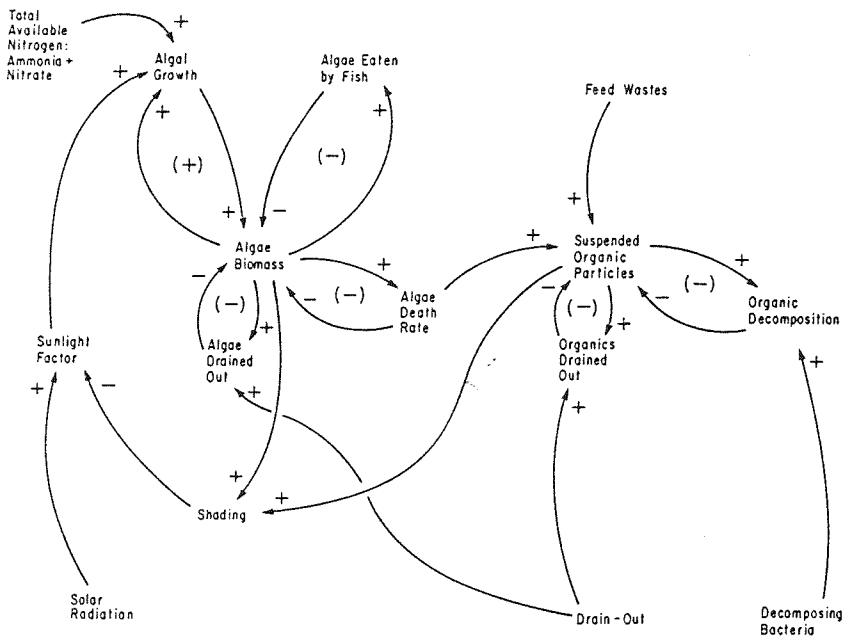

Fig. 6. Causal loop diagram of the algae sector.

hypothesis, is shown in Fig. 6. Algae biomass sits at the center of four simple feedback loops. One feedback loop is positive (algal growth) and three are negative (algae eaten by fish, algae drained out, and the natural algal death rate). The positive feedback loop describing algal growth is strongly affected by outside influences. At very low concentrations of ammonia and nitrate, nitrogen deficiency can reduce algal growth below its maximum potential. More importantly, the maximum growth rate is heavily regulated by how much light the average algal cell receives. This sunlight factor is defined by the incoming solar radition and the degree of 'shading', i.e. turbidity within the water column. Shading is in turn the sum of algal cells and suspended organic particles, the latter reaching concentrations much higher than the former. Suspended organic particles come from two sources: dead algal cells and feed wastes. Feed wastes originate in two ways: unassimilated feed and uneaten food. Both are a positive function of the feeding rate. Removal rates for suspended organic particles are also two-fold: decomposition and drain-downs.

The algae submodel is driven by five external factors: (1) solar radiation; (2) drain-out schedule; (3) feed wastes; (4) inorganic soluble nitrogen (ammonia and nitrate); and (5) decomposing bacteria.

The first two are truly exogenous variables, unaffected by any factors within the model. Factors (3) and (4) are strongly affected by another exogenous factor, the feeding rate, and are also influenced by factors in regions of the model outside the boundary of the algae submodel. The fifth, decomposing bacteria, is a factor generated internally by the larger model, and is also well outside the boundary of the algae submodel.

SUSPENDED ORGANIC PARTICLES SECTOR

Suspended organic particles play a key role in solar-algae pond dynamics. They act as a midway point in the decomposition process for both algae and feed wastes, before being broken down into inorganic constituents. The organic particles suspended in the water column shade living algae cells, hindering photosynthesis. The decomposition of the organics deteriorates water quality by consuming oxygen and generating toxic carbon dioxide and ammonia.

AMMONIA SECTOR

Ammonia is the first nitrogen breakdown product resulting from organic amine decomposition. Ammonia occurs in two forms, based on the number of hydrogen atoms bound to the nitrogen atom: un-ionized ammonia has the formula NH_3 and ionized ammonia is NH_4^+. While ionized ammonia is

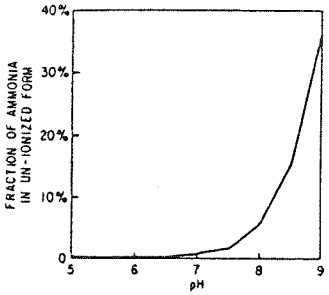

Fig. 7. The fraction of ammonia in its toxic un-ionized form as a function of pH.

mildly toxic to fish, un-ionized ammonia (NH_3) is extremely toxic. The proportions of the two forms is indicated by the pH of the water; the higher the pH, the greater the proportion of toxic un-ionized ammonia. Figure 7 illustrates the relationship between pH and the two forms of ammonia.

NITRITE (NO_2^-) SECTOR

Nitrite sits at the cross-roads of the transformation pathways for soluble inorganic nitrogen. Nitrite is the intermediate compound for both the nitrification and denitrification process. Nitrite is a molecule rich in energy potential for both processes: for nitrification, nitrite is an easily oxidized compound. For denitrification, nitrite is an oxygen-rich molecule, providing scarce oxygen with which to oxidize larger energy-rich molecules. For these reasons, nitrite is very ephemeral, and is usually present only in very small concentrations that belie the flow rate of nitrogen through this step. However, when nitrite is present, it is often deadly toxic to fish, turning red hemoglobin to brown methemoglobin that is incapable of releasing oxygen to the fish tissues (Bodansky, 1951). To complete the case that nitrite is the most transient and mysterious of the nitrogen compounds, its sharp toxicity is almost totally dulled in the presence of moderate salinity and conductivity. This toxicity inhibition mechanism is poorly understood, but definitely exists. Winter trials at New Alchemy comparing lightly salted to absolutely fresh ponds have shown the same inhibition of nitrite toxicity reported by others (Crawford and Allen, 1977; Perrone and Meade, 1977).

NITRATE (NO_3^-) SECTOR

Nitrate is the end product of nitrification; nitrifying bacteria oxidize ammonia to nitrite and then nitrate. The creation of ammonia, followed by

its nitrification, relies on oxygen. High concentrations of nitrate indicate a history of heavy aerobic decomposition accompanied by oxygen levels high enough to allow aerobic nitrification of the ammonia to follow. The only condition where high nitrate levels might not appear after such a pond history would be if strong algal photosynthesis assimilated the nitrate. On the other hand, little nitrate and persistent high ammonia concentrations suggest near-anaerobic conditions: the ammonia cannot oxidize to nitrite, and if it does it is more likely to then reduce to nitrogen gas, while any nitrate is also reduced to nitrite and then nitrogen gas. In an aged pond, then, with an accumulation of a large feed input, the presence or absence of nitrate can indicate whether the unassimilated nitrogen ultimately oxidized to nitrate or denitrified to nitrogen gas.

OXYGEN SECTOR

Oxygen profoundly affects both the health of the fish population and the ability of aerobic bacteria to operate. The concentration of oxygen influences fish growth directly through the fishes' physiology and indirectly by determining which water chemistry changes occur. Oxygen is depleted by many biological activities: fish respiration, decomposition, nitrification. It is replenished in two ways: through algae photosynthesis, and through invasion of atmospheric oxygen (as long as the water's oxygen concentration is below saturation/equilibrium with the partial pressure of oxygen in the air above).

CARBON DIOXIDE SECTOR

Except for the oxidation of ammonia and nitrite, every flow of oxygen has a corresponding flow of carbon dioxide moving in the opposite direction. Whereas oxygen is beneficial to fish, carbon dioxide is not — high concentrations of carbon dioxide in the water slow the release of carbon dioxide from the fishes' gills, in turn slowing the purge of carbon dioxide from fish tissues. Thus, in two ways, carbon dioxide acts as the mirror image of oxygen.

Carbon dioxide also has two unique characteristics:

(1) The air/water exchange of carbon dioxide is complicated by the fact that carbon dioxide does not just dissolve in water; it also reacts, forming carbonic acid and bicarbonate ions.

(2) Carbon dioxide, because it is reactive with water, plays a key role in the hydrogen ion activity of the pond (pH) and its acidity and alkalinity.

ALKALINITY AND pH SECTORS

Alkalinity is important to model because it, in combination with the carbon dioxide concentration, determines pH (and pH controls the relative

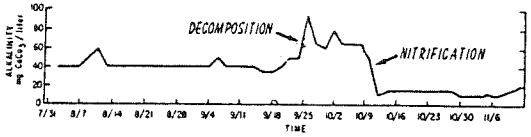

Fig. 8. Alkalinity changes in Pond H caused by decomposition and nitrification.

proportion of un-ionized and ionized ammonia). Alkalinity is the capacity to absorb acids without changing pH. Stumm and Morgan (1970) define alkalinity as:

$$(\text{alkalinity}) = (HCO_3^-) + 2(CO_3^{2-}) + (OH^-) - (H^+)$$

Alkalinity is typically measured in the buffering equivalent of $CaCO_3$. Carbonate, CO_3^{2-}, has the capacity to neutralize two hydrogen ions. Two hydroxyl ions have the same buffering capacity and therefore the same alkalinity, even though the molecular weight of the two hydroxyl ions is much less than the equivalent ion buffering capacity of one carbonate ion.

As Brewer and Goldman (1976) have shown, biological activity can change alkalinity. Strong changes in alkalinity can suggest the dominant biological process that is causing the alkalinity change. Figure 8 illustrates changes in alkalinity over time in Pond H. The most severe rise and dip in alkalinity are labelled 'decomposition' and 'nitrification', indicating the likely biological process driving the change.

Table 1, based on Brewer and Goldman's work, describes the specific biological and physiochemical reactions that can change alkalinity that are incorporated in the model.

TABLE 1

Alkalinity changes included in the model

Process	Reaction	Unitized alkalinity change	DYNAMO variable	Function of DYNAMO variable
Ammonia-to-algae [a]	$NH_4^+ > \text{orgN} + H^+$	−1	ALK1A	NITAG
Nitrate-to-algae [a]	$NO_3^- > \text{algN} + OH^-$	+1	ALK3A	NITAG
Decomposition [a]	$\text{orgN} > NH_4^+ + OH^-$	+1	LAK0A	OGAM
Respiration [a]	$\text{orgN} > NH_4^+ + OH^-$	+1	LAKF1	FSAM
Nitrification [a]	$NH_4^+ > NO_2^- + 2\,H^+$	−2	ALK12	AMNO2
Denitrification [a]	$NO_2^- > N_2 + OH^-$	+1	ALK2N	DENIT
$CaCO_3$ dissolution [b]	$CaCO_3 > Ca^{2+} + CO_3^{2-}$	+2	ALKIN	PH

[a] Biological process: based on Brewer and Goldman (1976, p. 115).
[b] Physical process: based on Stumm and Morgan (1970, pp. 11, 120–121, 130, 176–177).

BACTERIA SECTOR

Structure of the bacteria sector

The chemical transformation of nitrogen between organic amines, ammonia, nitrite, nitrate and nitrogen gas is intrinsically a biological process, accomplished by specific genre of bacteria. In the model, the five nitrogen transformations caused by bacteria are:

Decomposition / deammination

(1) The aerobic decomposition of organic matter and subsequent release of ammonia, caused by heterotrophic bacteria:

$$C_vH_wO_xN_y + (v + 0.25w - 0.5x - 0.75y)O_2 \rightarrow vCO_2 + (0.5w - 1.5y)H_2O + yNH_3 + \text{energy}\ *$$

Nitrification

(2) The oxidation of ammonia to nitrite, caused primarily by *Nitrosomonas* bacteria (Wetzel, 1975, p. 198; Sharma and Ahlert, 1977, p. 897):

$$NH_3 + 1.5\ O_2 \rightarrow H^+ + NO_2^- + H_2O + 66\ \text{kcal}\ *$$

(3) The oxidation of nitrite to nitrate, caused primarily by *Nitrobacter* bacteria (Wetzel, 1975, p. 199; Sharma and Ahlert, 1977, p. 897):

$$NO_2^- + 0.5\ O_2 \rightarrow NO_3^- + 18\ \text{kcal}\ *$$

Denitrification

(4) The reduction of nitrate to nitrite, caused by specialized anaerobic denitrifying bacteria (Hutchinson, 1957, p. 868; Wetzel, 1975, p. 201):

$$0.5\ CH_2O + NO_3^- \rightarrow NO_2^- + 0.5\ CO_2 + 0.5\ H_2O + \text{energy}\ *$$

(5) The reduction of nitrite to nitrogen gas, caused by a second group of denitrifying bacteria (Hutchinson, 1957, p. 868; Wetzel, 1975, p. 201):

$$0.75\ CH_2O + NO_2^- \rightarrow 0.5\ N_2 + 0.75\ CO_2 + OH^- + 0.25\ H_2O + \text{energy}\ *$$

Decomposition and nitrification ((1), (2) and (3)) are aerobic processes; the oxidation of the nitrogen-bearing compound yields energy directly. Denitrification ((4) and (5)) is an anaerobic process; the nitrogen compound provides oxygen atoms for the oxidation of energy-rich molecules.

All the bacterial sectors have an identical System Dynamics structure, although their coefficients differ. That structure is diagrammed in Fig. 9.

* In the strict thermodynamic convention, net energy generated by moving the reaction from left to right should be represented by a *negative* energy value on the right-hand side.

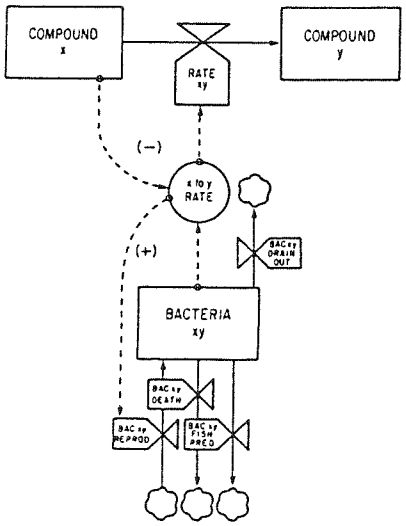

Fig. 9. The basic structure of the bacterial/chemical transformation system, showing the two major feedback loops, one negative and one positive.

The structure contains one profoundly powerful positive feedback loop that links bacterial growth with chemical transformation: the greater the rate of chemical processing, the more energy is captured by the bacteria for biomass accretion and reproduction. The more bacterial biomass, the greater the chemical processing capability. The chemical process not only generates bacterial growth, it also depletes the original compound, thereby creating a strong secondary negative feedback loop. This coupling of strong positive and negative feedback loops make the original compound disappear quite suddenly, matched by an equally sudden appearance of a new compound (see Fig. 10).

Since the chemical transformations are linked in series, both the nitrification and removal of the compounds tend to be exponential. Thus the compounds have a strong tendency to 'spike' and disappear again.

If the bacteria have no energy substrate upon which they can continue to work, the bacteria gradually decay exponentially to zero, due to various bacterial removal rates. The removal rates are threefold:

(1) natural bacterial senescence and cell lysing;

(2) physical removal through (a) water replacement, and/or (b) particulate filtration;

(3) predation by tilapia that filter and ingest the particulates upon which bacteria flourish.

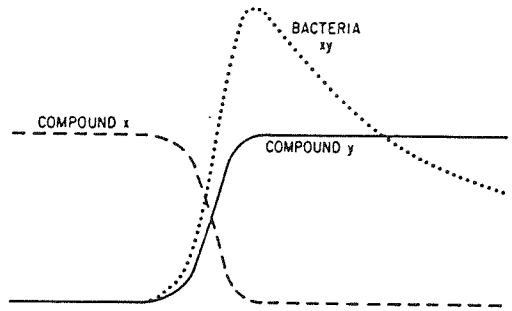

Fig. 10. The strong positive feedback between bacteria and water chemistry generates sudden changes in both.

Removal rates (2b) and (3) presume that the bacteria are primarily associated with particulate substrates, making the bacteria susceptible to particulate filtering. This is undoubtably true for heterotrophic bacteria that act directly on the particulate matter. This concentration on particulates is also likely for nitrification bacteria, since nitrification is enhanced by the addition of explicit surface area, also provided by particulate matter. The clustering phenomenon is also probable for denitrifying bacteria, since adherence to bottom sediments would reduce the likelihood of being washed upward into oxygen-rich waters unfavorable to anaerobes.

EXOGENOUS VARIABLES SECTOR

Exogenous variables affect elements within the model, but no feedback returns to affect them. They are therefore independent variables that tend to 'drive' the system. Some exogenous variables can be readily controlled (though their use may exact an energetic or materials cost); these include the feeding rate, drain-down schedule and aeration. Others, such as solar radiation cannot be easily controlled. Specifically, solar radiation can only be altered by reducing its input through shading, or increasing it slightly and with difficulty by adding reflectors.

Feeding schedule

The 100-day feeding schedule for Pond H is entered in the table called FEED1T. The trout pellet weight is then converted to its absolute dry weight (the feed is 92% dry). The total feed input is accumulated in the level called FED. In rerun mode, an alternative feeding regime can be input on a daily basis through FEED1T or on a biweekly basis with FEED2T. The switch from one to the other is controlled by FSW (the Feeding Switch).

Solar radiation data

Daily solar radiation is usually measured as the daily total of light energy striking a horizontal surface, and typically has the units Ly/day or cal cm^{-2} day^{-1} *. These data cannot be used directly to infer the amount of light entering a solar-algae pond; the light striking a horizontal surface will not be directly proportional to the light entering through the side walls of a cylindrical fiber-glass solar-algae pond. The ratio of direct/diffuse sunlight changes from cloudy to sunny days, and the path of the sun across the sky changes through the year. Both of these factors affect the angle of incidence of light onto the various pond surfaces, and this affects the percentage of light that is transmitted to the water column. This necessitates a secondary model that translates horizontal daily radiation into the amount of sunlight that actually penetrates the top and sides of the pond. The program that performs this translation is called SOLAR6. The program is quite complex, taking into account direct and diffuse radiation, as well as the complex reflection patterns in the reflective solar courtyard in which the experimental ponds sit. The model keeps track of the angle at which all these light sources strike all the surfaces of the cylindrical pond (both curved sides and horizontal top), and uses a nonlinear function to calculate the light transmission according to the angle of incidence. SOLAR6 is written in the FORTRAN computer language; the code appears at the end of Progress Report 4, pp. 66–70. Many of the concepts in SOLAR6 are based on Duffie and Beckman's textbooks on solar engineering (1974, 1980). Meterological data are drawn from Payne's (1978) monthly climatological sheets for Woods Hole. Descriptions of various evolving stages of the model appear in Progress Report 1 (pp. 51–64, note: Fig. 10 on p. 55 is in error), Progress Report 3 (pp. 97–99), and Journal 6 (Wolfe et al., 1980, pp. 100–103; see in particular Figs. 1 and 2 describing the reflected radiation patterns).

Using the sunlight transmission program SOLAR6, daily totals for horizontal solar radiation were used to extrapolate the total amount of solar radiation penetrating the pond surfaces and entering the pond water column.

Water exchange schedule

The simplest method to upgrade water quality is to exchange old pond water with fresh water. Drain-downs and water replacement effectively

* Ly, langley = 1 cal cm^{-2} = 41.868 kJ m^{-2}.

remove at least an equivalent fraction of algae, suspended organic particles and soluble inorganic nitrogen compounds (ammonia, nitrite and nitrate). Because the incoming water is typically aerated, it is near atmospheric equilibrium in both oxygen and carbon dioxide. Thus water replacement will have a minimal impact on the concentration of these dissolved gases. In the standard run experiment, 20% of water volume was typically exchanged each week.

Aeration

Aeration is the fourth significant exogenous variable. Aeration affects the ability of gases to cross the air/water interface. In the model, the three gases that explicitly cross this interface are un-ionized ammonia, oxygen and carbon dioxide. Nitrogen gas generated by denitrification also passes out across the interface, but its dissolved form does not significantly affect other biotic or abiotic factors in the model, so while the generation of nitrogen gas is modelled, the destiny of the gas is not.

The escape rate for any gas across the water/air interface is:

$$\frac{\text{diffusion coefficient} * [\text{gas in water} - \text{gas saturation in water}]}{\text{depth of pond} * \text{air/water interface film thickness, } f(\text{aeration})}$$

The advantage of this formulation is that once the air/water interface film thickness is determined, the air/water exchange rates can be predicted for any gas, using the diffusion coefficient unique to the particular gas in question. The diffusion coefficients for several gases are listed by Broeker (1974, p. 127). Broeker does not specifically list the diffusion coefficient for ammonia, but points out that the diffusion coefficient is inversely proportional to molecular weight. The value for ammonia is thus inferred from the values listed for hydrogen, helium, neon, nitrogen, oxygen, argon and carbon dioxide gases. Broeker lists the diffusion coefficients in the units 10^{-5} cm^2/s. Table 2 converts Broeker's values to cm^2/day.

TABLE 2

The diffusion coefficients for the three gases simulated in the model

Gas	Diffusion coefficient	
	(10^{-5} cm^2/s)	(cm^2/day)
NH_3, ammonia	3.2	2.8
O_2, oxygen	2.3	2.0
CO_2, carbon	1.9	1.6

TABLE 3

Time coefficients and the corresponding interface film thickness for a range of aeration conditions

Condition thickness	Time coefficient		Film (cm)
	(h^{-1})	(day^{-1})	
Still air	0.007	0.17	0.08
Wind	0.025	0.60	0.023
Poor aeration	0.12	2.90	0.005
Good aeration	1.6	38.0	0.00036

The air/water interface film thickness through which the gas must diffuse varies according to windspeed across the pond surface and aeration. The diffusion coefficient divided by the pond depth and film thickness will yield another coefficient, k, describing the exchangability for a particular gas, and having the dimensions 'per unit time'. This coefficient k was determined for oxygen in an abiotic solar-algae pond under several wind and aeration conditions, and reported in Progress Report 2, p. 14. The k coefficient can be converted to the film thickness in the following manner:

k = diffusion coefficient/(depth * film thickness)

thus film thickness = diffusion coefficient/(k * depth). In Table 3, the per hour coefficients are converted to generic film thicknesses.

SIMULATION RUNS OF THE MODEL: INTRODUCTION

The DYNAMO flow diagram shown in Fig. 1 at the beginning of this paper symbolically represents the equations that precisely define the relevant causal relationships in the solar-algae pond ecosystem. This set of equations is the 'model'. A 'simulation run' of the model is a series of calculations dictated by the model. A simulation run starts with specified initial values and then computes all the variables for every tiny 'DT' step through time according to the rules set forth by the model. Each simulation run looks at a particular set of initial values, assumed parameters and exogenous variables impinging on the model. Each simulation tracks all 14 levels, 55 rates and 44 auxiliary variables illustrated in Fig. 14 (not to mention the several dozen supplementary variables that act as indicators, and are not diagrammed). Thus, one simulation run can generate an enormous number of plots of different variables in the model.

THE STANDARD REFERENCE RUN

Any model of a complex nonlinear feedback system needs to be tested against observed time series data. Unless a good match is made, the reliability of the simulation when extrapolating to untested situations remains in grave doubt. The model described heretofore successfully reproduces the absolute levels and transient dynamics of a broad range of variables observed in three intensively monitored solar-algae ponds during the late summer and fall of 1978. The three ponds are labelled H, J and L, denoting their position in the reflective solar courtyard adjacent to the Cape Cod Ark. Pond H and L were fed high-protein trout pellets, while Pond J was fed rabbit pellets with a lower nitrogen content.

How to read a DYNAMO plot

Figure 11 depicts the major indicator variables simulated in the standard run of Pond H. The horizontal axis of the graph represents time, and extends from day 0 to day 98 (14 weeks). Several variables are plotted across

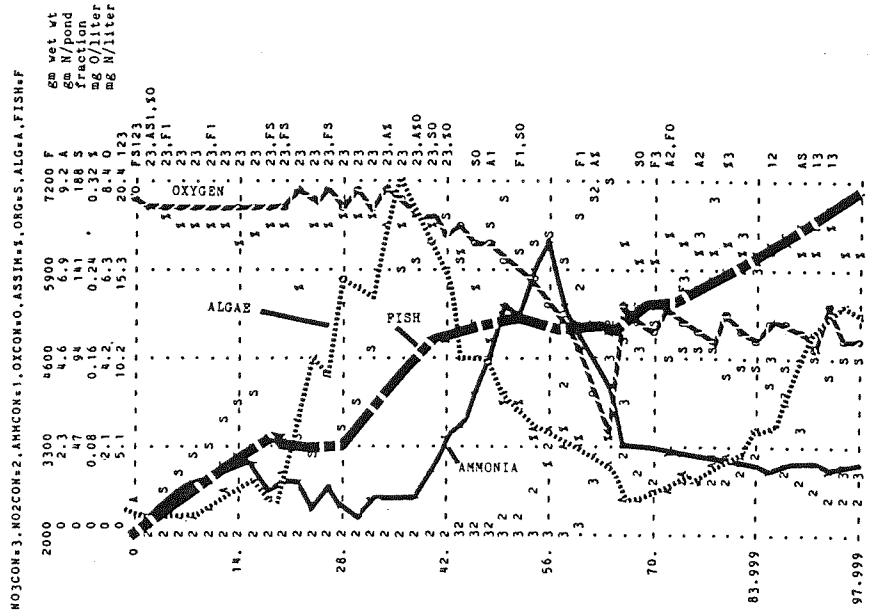

Fig. 11. Pond H standard run; the major indicators—fish biomass, algae density, ammonia and oxygen.

time; each has its own vertical scale. Each variable is represented by a character; the translation from variable name to character is given in the leftmost line. In this case it reads: NO3CON = 3, NO2CON = 2, AMMCON = 1, OXCON = 0, ASSIM = %, ORG = S, ALG = A, FISH = F.

This line says that the nitrate concentration (NO3CON in the model, with the units mg N/l) will be represented by a '3' on the plot, nitrite by a '2', etc. The next several lines, just to the left of the actual plot, give the scales for each variable. Fish biomass ranges from 2000 to 7200 g, algae scale from 0 to 9.2 g N/pond, suspended organic particles (S) range from 0 to 188 g N/pond, the assimilation fraction scales from 0 to 0.32, oxygen scales from 0 to 8.4 mg/l, and the soluble inorganic compounds ammonia, nitrite and nitrate (1, 2, 3) range from 0 to 20.4 mg N/l. The computer automatically adjusts the top of each scale to equal or slightly exceed the highest value of that particular variable; occasionally for comparative purposes the scales are held fixed from plot to plot. It is extremely important to always examine the scale of values when comparing different plots. For instance, the standard plots of Pond H, J and L (Figs. 11, 23 and 24), have significantly different ranges (note in particular the fish biomass, algae, suspended organics and nitrogen compounds scales).

Examination of the Pond H standard simulation run

Knowing how to read a DYNAMO plot, we can now interpret Fig. 11. Remember that Fig. 11 shows only eight of the nearly 200 variables computed in this simulation run. The fish biomass grew rapidly initially, and then stopped at a short plateau during an influx of ammonia. Since pH was relatively high, much of the ammonia was in its toxic un-ionized form. Vigorous algal growth assimilated this ammonia, simultaneously generating oxygen and removing carbon dioxide. All these influences of the algae on water quality created healthier conditions for the tilapia, and rapid fish growth resumed. Meanwhile, feed wastes (both uneaten and unassimilated) and dead algal cells accumulated in the water column as suspended organic particles. Eventually they severely shaded the algae, and the algal population collapsed from insufficient solar energy input. As the algae faltered, the decomposing bacteria were concurrently becoming strongly established. Without the ameliorating influence of algal growth, the full impact of decomposition on water quality was felt. Ammonia and carbon dioxide shot upwards, oxygen plummeted. Fish growth stopped abruptly. As the nitrifying bacteria became established, they oxidized the ammonia to nitrite, also extremely toxic to fish. This prolonged the plateau that the fish biomass had reached. Then most of the nitrite denitrified to harmless nitrogen gas, while a smaller fraction oxidized to nitrate (also quite benign to fish). The carbon

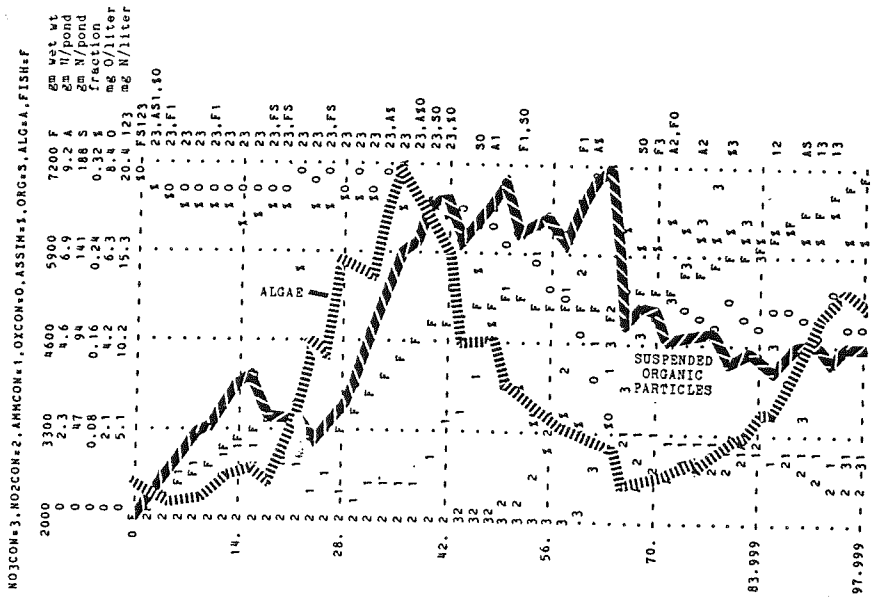

Fig. 12. Pond H standard run; the relationship between algae and suspended organic particles.

dioxide plateaued, while oxygen actually recovered. Concurrently, the bacteria in all five functional groups increased exponentially to major concentrations, while the algae began a slow come-back as the suspended organics disappeared through decomposition. The increased water quality, combined with the influx of microbial feeds, spurred a third climb in fish biomass.

The preceeding interpretation goes into more depth than the information given in Fig. 11; it is also based on plots of other variables for the same set of conditions. These plots are shown subsequently in Figs. 12 through 16.

The relationship between the algae and suspended organic particles is shown in Fig. 12. The algae, initially thwarted by strong tilapia predation and scant nutrient concentrations, began to grow rapidly as the initial limiting factors disappeared (algae species resistant to tilapia predation became established, and respiration and decomposition brought nutrient levels to nonlimiting concentrations). Simultaneously, suspended organics particles accumulated, generated by senescent algal cells and particularly by fish feed wastes. During the 6th week, the organic particles reached densities of shading that made the algae population unsustainable. The algae declined precipitously. The suspended organic particles maintained high densities and

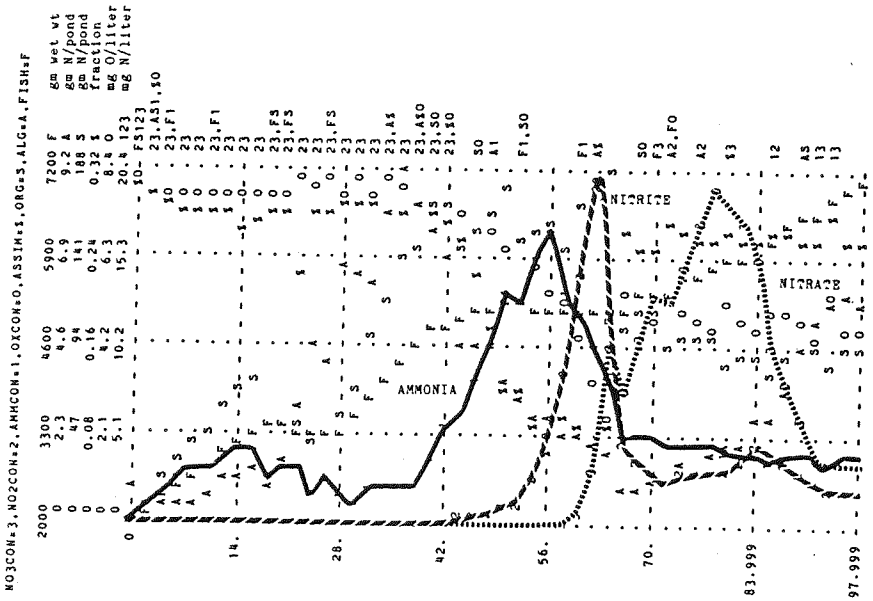

Fig. 13. Pond H standard run; the soluble inorganic nitrogen compounds—ammonia, nitrite, and nitrate.

continued to suppress algal growth for many weeks. However, the decomposing bacteria simultaneously established themselves. The decomposers oxidized the organics to virtually colorless and invisible inorganic constituents (carbon dioxide, water, ammonia, phosphate). The decomposers exponentially grew to densities that finally forced the suspended organic particles to decline. The reduced shading allowed a recovery of algal populations during the final 4 weeks of the experiment.

Figure 13 depicts the soluble inorganic nitrogen compounds: ammonia, nitrite and nitrate. The three successive peaks suggest a smooth transition from ammonia to nitrite and then nitrate; a textbook picture of nitrification (for instance, see Collins et al., 1975) for an observed, smooth nitrification transition). In fact, the observed Pond H data match the ammonia peak, but fail to display the subsequent nitrite and nitrate peaks shown in this simulation. Either the empirical measurements, or the modelling, of nitrite and nitrate are inaccurate. The sharp narrow peak of nitrite could have been missed entirely by the weekly measurement interval. Also, high nitrite/nitrate ratios can lead to imprecise measurements of nitrate. However, none of these measurement errors could alter nitrite or nitrate concentrations by more than 2 mg N/l. Alternatively, and much more likely, the measured nitrite

and nitrate values are correct, and a complicated interaction between nitrification and denitrification caused the irregular pattern of nitrite and nitrate in the last 6 weeks of the experiment. The shifts would depend heavily on oxygen, pH and bacterial interactions whose essence is not quire captured by the present model. Fortunately, at the end of the experiment the nitrite's toxicity is almost certainly heavily moderated by various salts, so the question of whether the nitrogen is in the form of nitrite or nitrate probably has little impact on fish growth. Also, the simple succession of ammonia to nitrite and then nitrate simulated in Fig. 13 has been observed in wintertime ponds.

The authors speculate that there might be an alternative causal structure which could mote closely fit the complex ammonia, nitrite and nitrate pattern. The question lies in whether there actually are five distinct bacterial groups or could one group perform more than one function? Indeed, it is possible that heterotrophic bacteria (that generate ammonia) could become facultative anaerobes, using nitrate and nitrite as electron acceptors to continue oxidizing energy-rich organic molecules (Brock, 1979, p. 113). This anaerobic process is denitrification. Such an ability would be selectively advantageous, since strong aerobic decomposition frequently causes anoxia. If the heterotrophic decomposers are facultative denitrifiers, then strong denitrification could occur directly after decomposition, with no delay for a second bacterial group of functionally-specific denitrifiers to grow and become established. This could readily explain anomalous nitrogen activity in all the summer ponds: after the major ammonia peak, all soluble inorganic nitrogen disappears. It is not until 2 weeks later that nitrite and then nitrate begin to appear. The mysterious 2-week period of little nitrogen occurs while oxygen plummets to its lowest values. If the decomposers can shift to denitrification, then any conversion of ammonia to nitrite would be followed immediately by denitrification of that ammonia, and both ammonia and nitrite would be diminishingly small. As oxygen recovered, denitrification would slow, nitrite could accumulate, and nitrate-producing bacteria could eventually begin to oxidize the nitrite to nitrate. Given the anomalous observed data, the possibility that decomposers largely displace specific denitrifiers is quite plausible. Restructuring of the model to explore this change will occur during the next stage of the modelling effort.

Figure 14 depicts the growth of the five separate functional groups of bacteria presently assumed by and simulated in the model. The bacteria do not reach significant concentrations until the second 7 weeks of the experiment, after the algae has peaked and then declined. Thus the shift from algal dominance to bacterial dominance is readily seen here. The decomposing bacteria (1) are the pioneers, followed by the nitrifiers (2 and 3), and finally the denitrifiers (4 and 5). Observed data indicates most of the denitrification

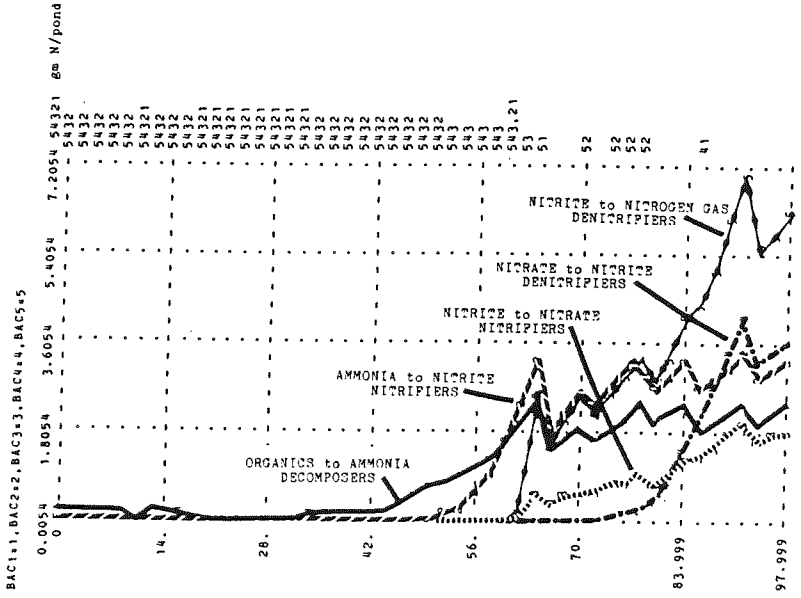

Fig. 14. Pond H standard run; bacterial growth.

may actually be performed by decomposers, thereby allowing denitrifying activity to occur concurrently with nitrification, rather than following nitrification. If bacterial groups 4 and 5 were incorporated into group 1, the succession would simply be 1, 2, 3.

Figure 15 shows the relationship between the feed assimilation fraction and fish growth. During the 8th and 9th weeks the assimilation fraction declined precipitously due to poor water quality, and fish biomass during this period plateaued. This plateau was actually the second time fish growth stagnated. The first fish biomass plateau, during the 4th week, is not as well explained by the brief dip in the asimilation fraction. Instead, one must examine the feeding schedule. Because of concern about high un-ionized ammonia concentrations, feeding was discontinued at the end of the 3rd week. During the 4th week, the fish were only fed on one day. The first plateau, then, was caused primarily by the low feeding rate, and not the fraction of feed that could be assimilated.

The model also tracks the fate of every gram of nitrogen in the pond ecosystem. Figure 16 plots the sinks where the nitrogen accumulates. Fish biomass begins as the primary reservoir of nitrogen. As feed inputs increase the nitrogen in the ecosystem, the excess nitrogen accumulates primarily as suspended organic particles. Water drain-downs (replaced with fresh water)

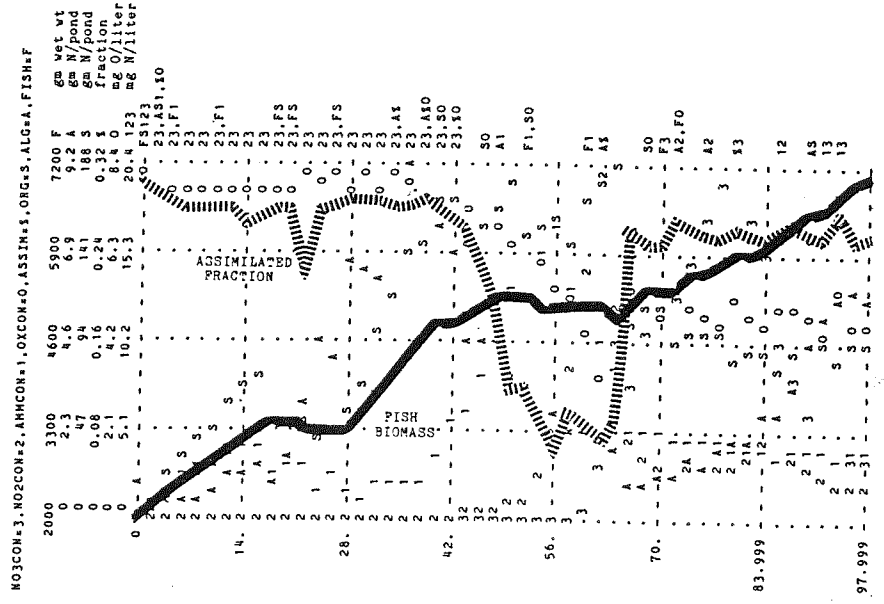

Fig. 15. Pond H standard run; the relationship between the assimilated fraction of ingested feed (ASSIM) and fish biomass.

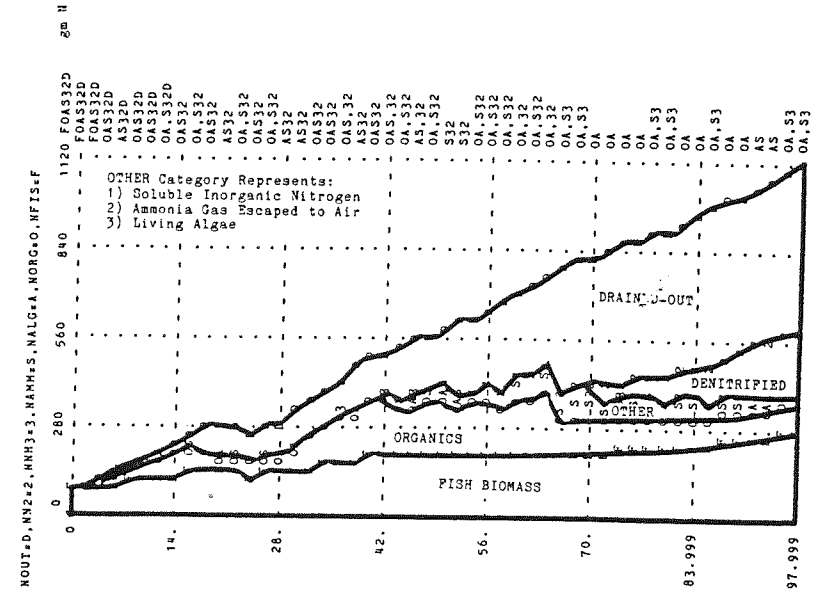

Fig. 16. Pond H standard run; nitrogen accumulation.

remove a large fraction of the input nitrogen. This eventually accounts for more than half of the feed nitrogen input. A sink for nitrogen that became significant towards the end of the experiment was the loss of nitrogen through denitrification to nitrogen gas. Roughly 15% of the input feed nitrogen eventually was lost to denitrification. In the middle of the experiment, the 'other' category of nitrogen appeared to have its greatest proportional impact. This category has three components: (1) soluble inorganic nitrogen compounds (ammonia, nitrite and nitrate), (2) ammonia gas that has escaped to the atmosphere, and (3) living algae. Ultimately, even the combination of all three categories cannot rival the magnitude of the four previously mentioned categories (fish biomass, suspended organic particles, denitrification and drained-out nitrogen).

Comparison of simulated and observed data for Pond H

Figures 17–22 display observed and simulated variables on the same plot. The first four figures compare the primary indicator variables shown initially in Fig. 11: fish biomass, algal biomass, oxygen and ammonia. As shown in Fig. 17, the simulated values for fish biomass fall well within the 95% certainty band for all the fish weight samplings that took place, with the

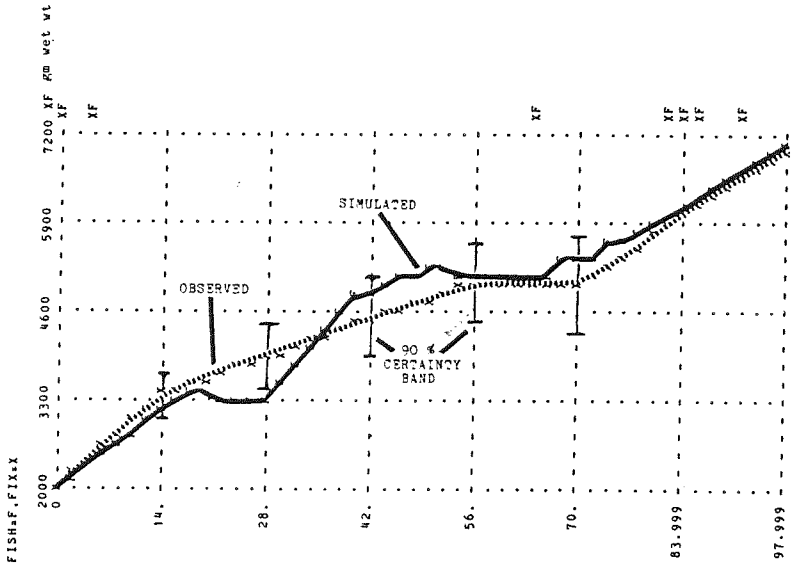

Fig. 17. Pond H standard run: simulated versus observed fish biomass.

exception of day 28. This higher observed value negates the simulation's prediction of a fish growth plateau caused by the feeding stoppage during the 4th week. The fish biomass predicted by the simulation for day 28 does easily fall within a 90% certainty band. However, if the simulation does significantly underestimate fish biomass at day 28 (and slightly at day 14), it may indicate that the initial microbial populations actually make an even greater contribution to tilapia nutrition than the model predicts. This buttresses the model's contention that microbial feeds do have a significant impact.

Figure 18 compares observed and simulated algal biomass. For Figures 18–22, week-long averages are plotted, omitting some of the 'jumpiness' in the graph of variables shown in Progress Report 3. The simulated and observed values match quite closely. This is well within the range of certainty for algae nitrogen extrapolated from algal biomass that in turn is based on species-disaggregated algal cell counts.

Figure 19 compares simulated and observed oxygen concentrations. The comparison made here is deceptive: the observed values are for midday (13 : 00 h) readings, while the simulated values represent all-day averages. Thus, only trends should be compared. Both simulated and observed oxygen values dip sharply at the identical time (day 64). The observed oxygen values

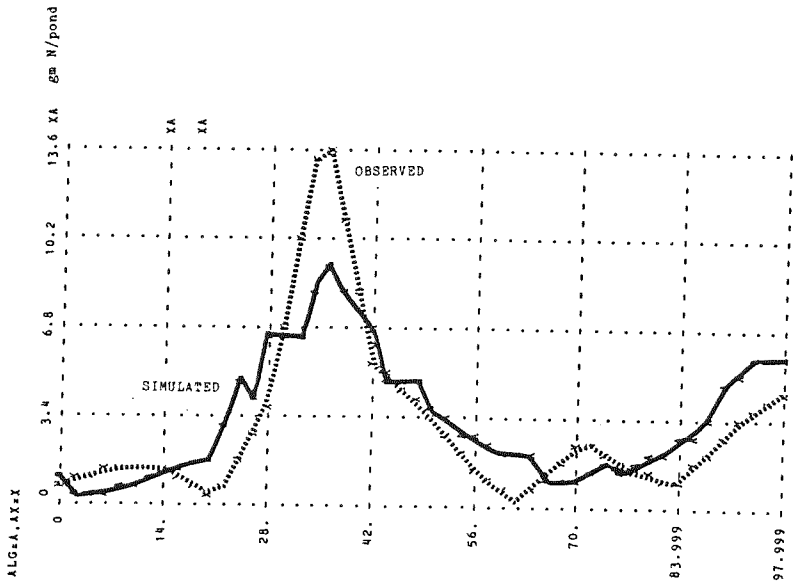

Fig. 18. Pond H standard run: simulated versus observed algal densities

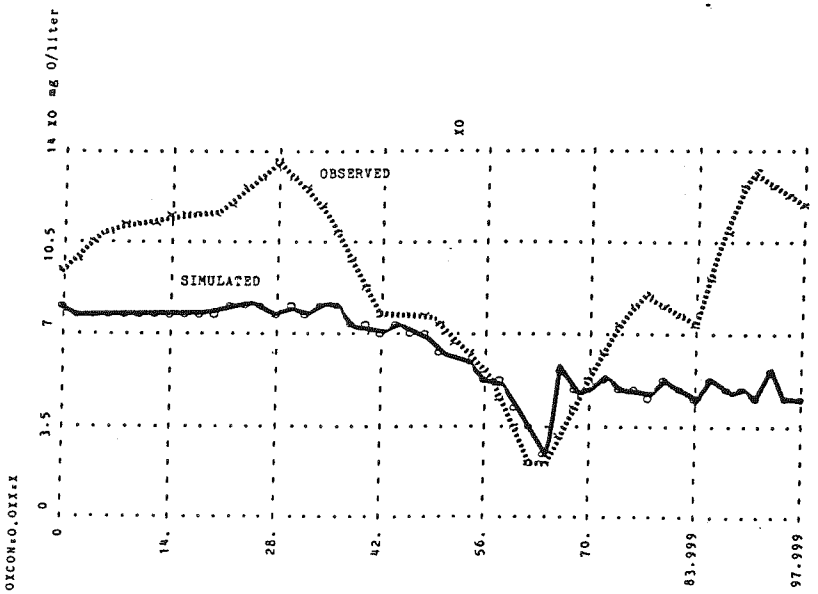

Fig. 19. Pond H standard run; simulated all-day average oxygen concentration versus midday observed oxygen levels.

rise sharply thereafter in an intriguing manner. Examining the algal cell counts graphed for Pond H in Progress Report 3 reveals that spikes of a very small *Chlorella* (mislabelled *Oocystis* in Progress Report 3) occurred at the same time. These small *Chlorella*, though very numerous, amounted to insignificant biomass densities. Two hypotheses are possible: (1) the model underestimates the photosynthetic rate per unit of algal biomass when the algal cells are very small, or (2) the high midday oxygen values are offset by lower nighttime values, and the moderate simulated oxygen values for the last 4 weeks are reasonably accurate. A combination of both hypotheses probably come closest to fitting reality. Disaggregating the algae into large and small cells with different photosynthetic/respiratory rates would certainly be difficult. For instance, it is not clear what conditions would grant one size of algae a selective advantage over another, since tilapia predation intensity is relatively constant.

Ammonia is a key indicator of the decomposition of organic matter. The basic small peak, trough, big peak trend in the observed data is captured in the standard simulation run for Pond H. This is shown in Fig. 20. Differences do exist between the observed and simulated peaks, however. For the first peak, the observed data indicates a greater initial influx of ammonia

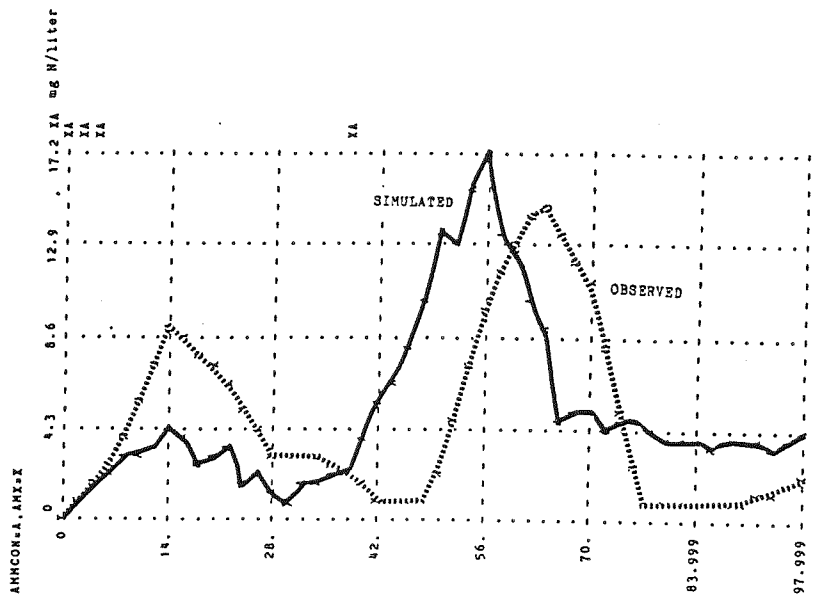

Fig. 20. Pond H standard run; simulated versus observed total ammonia.

than the simulation predicts. Apparently the model is sequestering the nitrogen as suspended organic matter, while in reality slightly more ammonia is being released through immediate decomposition. The simulated second peak precedes the actual peak by several days. Here the opposite condition seems to exist: in reality the suspended organic matter is more refractory than the model suggests. A more precise fit might be accomplished if the organic matter was divided into two categories: readily decomposed, and relatively refractory. The initial peak would be higher, because of the immediate ammonia release from the easily decomposed material, while the second peak would be delayed because the remaining material would be more difficult to break down, and might require a second bacterial group to transform the material to the readily decomposed form.

Alkalinity changes are tied rather closely to the same basic processes that caused the second ammonia peak and decline: decomposition causes an increase in both ammonia and alkalinity, while nitrification causes a decrease in both. Whereas alkalinity is generally thought of as un unchanging property, Fig. 21 reveals the dynamic nature of both the observed and simulated alkalinity. Because alkalinity and ammonia respond similarly to decomposition and nitrification, a clear parallel exists: in both cases, the simulated major peak precedes the actual observed data by approximately

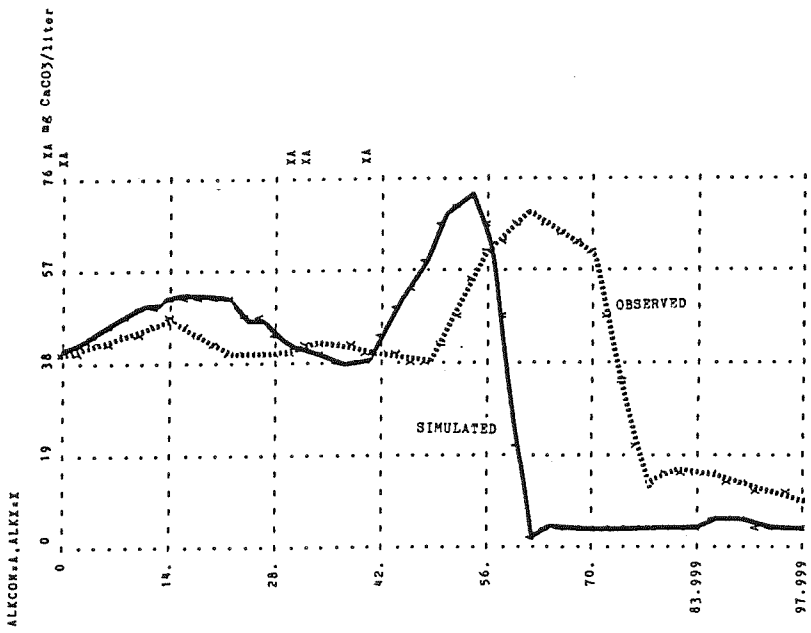

Fig. 21. Pond H standard run; simulated versus observed alkalinity.

Fig. 22. Pond H standard run; simulated versus observed pH.

one week. Figure 22 compares simulated and observed pH. Alkalinity strongly influences pH, and a combined look at Figs. 21 and 22 suggest that if alkalinity were slightly more precisely modelled, then the simulated pH trend might match observed data more precisely too.

In summary, the simulated data fits the observed data quite sufficiently, capturing the essential dynamics and usually staying within the bounds of measurement error. Where the simulation strays from observed data, a closer fit cannot be attained without significantly increasing the structural complexity of the model, and therefore the costliness of using the model. In the author's opinion, the essential dynamics are well-captured, and the model can be extrapolated to untested situations in order to gain insights into designing and managing the solar-algae ponds to produce more fish more efficiently.

Simulating other experimental regimes: Ponds J and L

Two other ponds located in the solar courtyard during the same period as Pond H were closely monitored and then simulated: Pond J and Pond L. Pond J was fed rabbit pellets while Pond H was fed trout chow.

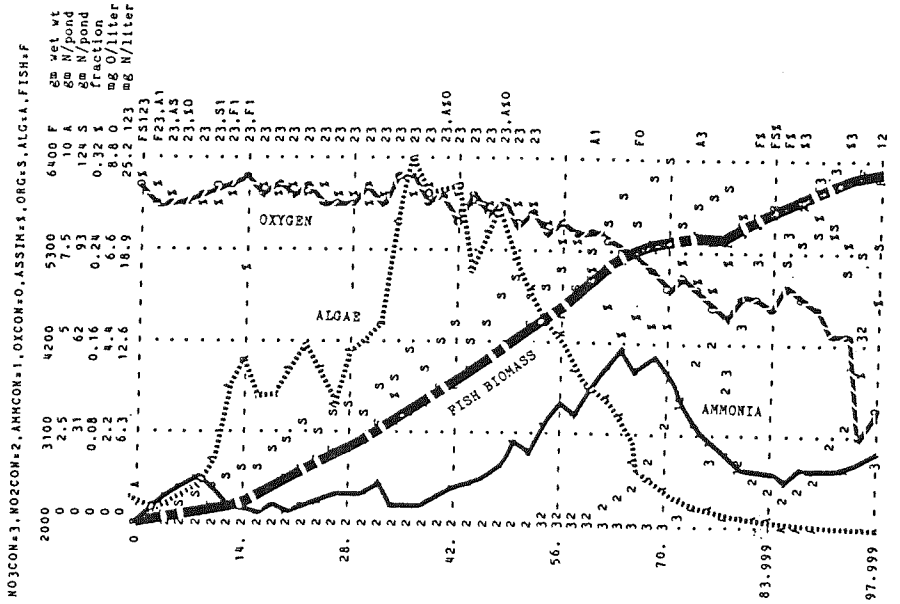

Fig. 23. Pond J (fed low-nitrogen rabbit feed).

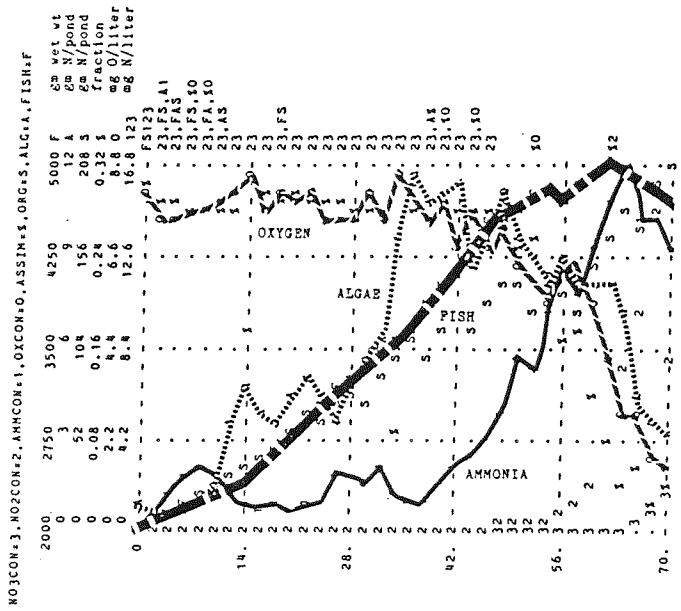

Fig. 24. Pond L (tsting for internally generated versus externally imposed decline in fish biomass).

The results of the parameter changes to fit Pond J's conditions are plotted in Fig. 23. When these simulation results are compared to the graphs of measured data detailed in Progress Report 3, the fish biomass and algae biomass match quite closely. The simulated ammonia concentrations fit the observed data up to about day 56, when the actual ammonia concentrations decline while the simulated ammonia concentrations persist for another two weeks before falling.

Pond L is a special case: around day 45 the airline leading to this pond was disconnected, presumably by an unsupervised visitor who accidentally tripped over the exposed tubingh. On days 47–52 mortalities decimated the fish population. The parameter changes above match the actual situation in all ways except for this accidental discontinuation of aeration. The objective was to see if the pond's own internal dynamics were leading to a severe decline in water quality at this time anyways. The answer is shown in Fig. 24. It suggests that a serious deterioration in water quality would have occurred around day 70 if the aeration disruption had not occurred. This simulation suggests that the mortality was triggered entirely by external conditions; the internal dynamic alone would not have caused the poor water quality conditions at day 50.

SIMULATION RUNS TESTING MANAGEMENT AND DESIGN CHANGES

Feeding rate

One of the most easily controlled variables with a profound impact on the ecosystem is the exogenous feed input. In the Pond H experimental run, the feeding input was irregular, and often exceeded the fish population's appetite satiation limit. This is shown in Fig. 25, where the satiation limit and the feeding rate are plotted together. If the same total amount of feed was introduced using a more consistent and even feeding rate, much better growth occurs. The even feeding rate increases fish growth 17%. As shown in Fig. 26, it is apparent that the feeding rate does not approach the satiation limit much of the time. Thus another run was made, increasing the feeding rate during those periods when the fish would accept the feed. Note there is some positive feedback between the feeding rate and the appetite limit (feeding increases fish biomass, which in turn increase the fish population's capacity to accept feed). Thus, in Fig. 27, both the feeding rate and the satiation limit have increased. Even more growth occurs, although the food conversion ratio declines a bit because the increased feed input does have a

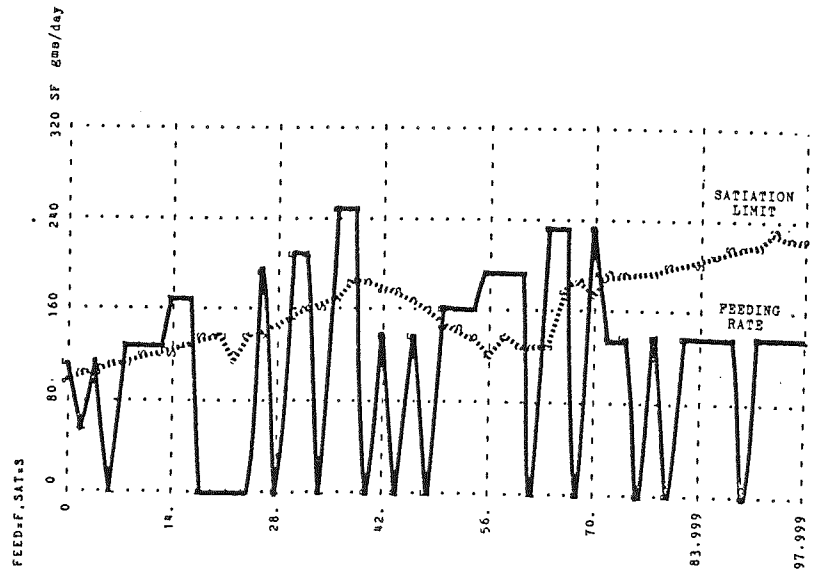

Fig. 25. Pond H standard run; irregular feeding rate compared to the fish population's [illegible] satiation limit

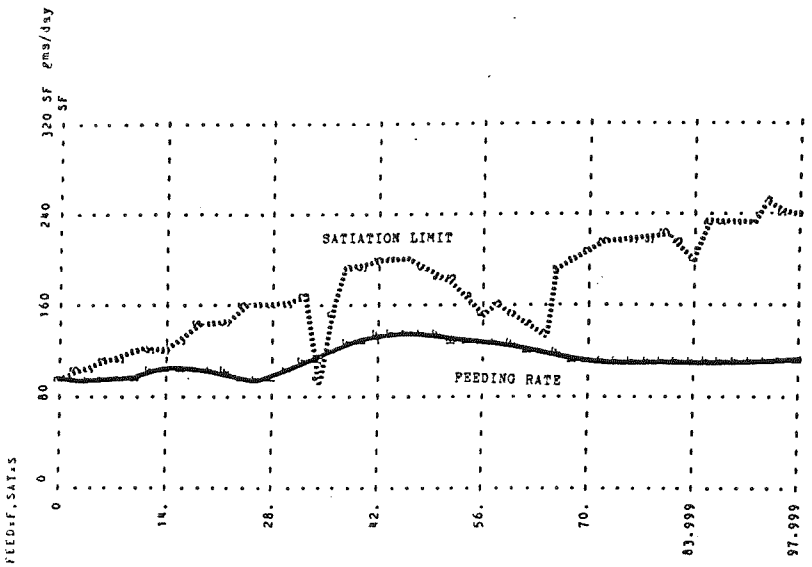

Fig. 26. Pond H with an even feeding rate (2-week averages equal the standard run) compared to the fish population's appetite satiation limit.

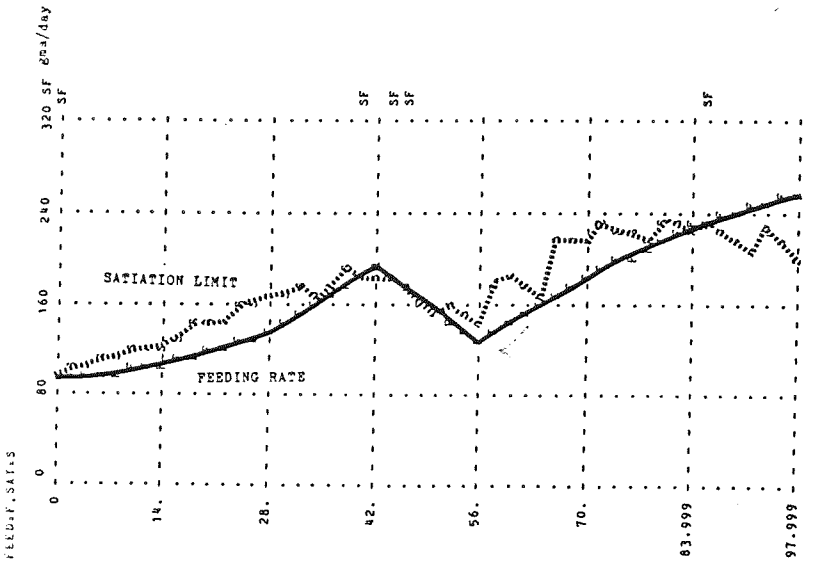

Fig. 27. Pond H with an enhanced, even feeding rate compared to the fish population's appetite satiation limit.

TABLE 4

The effect of the feeding regime on fish growth

Case	Total feed input	Total fish growth	Food conversion ratio
Standard run, irregular feeding	11.1	5.03	2.21
Even feeding equalling standard run	11.1	5.86	1.89
Even feeding, increased total input	16.1	6.89	2.34

negative impact on water quality. The feed input, fish growth and food conversion ratios for all three situations are shown in Table 4.

In summary, Table 4 demonstrates the beneficial effects of feeding tilapia as regularly as possible, and in most cases, as close to their appetite satiation limit as possible, without ever exceeding that limit.

Differing fish populations with equal feed inputs

The average fish size and total biomass affect how a given feeding rate influence water quality and fish growth. Larger fish have lower respiration rates per body weight. This lowers their appetites proportionally, and allows them to set aside more feed energy for growth or reproduction, instead of maintenance respiration. The model assumes that no breeding took place in the upright solar-algae ponds. This assumption has some basis in fact; we have observed that a solar-algae pond is an environment that generally discourages reproduction. Table 5 summarizes simulation run results predicting the fish growth for eight different tilapia populations, where the feed input rate is constant across the board.

TABLE 5

Fish growth under equal feeding regimes for eight different tilapia populations (varying gish size and total biomass)

	Daily feed/ biomass percent (bwd)	Total fish biomass	Average size of individual fish			
			20 g	40 g	80 g	160 g
	2%	4 kg				
Fish pop			200 f	100 f	50 f	25 f
Fish growth			3.2 kg	3.9 kg	4.5 kg	4.9 kg
	4%	2 kg				
Fish pop			100 f	50 f	25 f	13 f
Fish growth			4.9 kg	5.3 kg	5.7 kg	5.7 kg

As Table 5 illustrates, the larger fish grow more efficiently, all other factors being equal (feeding rate, total fish biomass, and bwd). Feeding the same absolute rate to a smaller fish population yields a larger initial feed/biomass fraction, or 'bwd' (body weight fed daily). At 4%, the feeding rate does not initially exceed the satiation limit (except, perhaps, for the very large fish). Since respiration percentage is unchanged for a given fish size, more feed energy is left over for growth, and the 4% bwd feeding rate proves more effective than the 2% bwd, if all other things remain equal (i.e., average fish size and absolute feeding rate).

Aeration

The effectiveness of the aeration system is described by coefficients defining the thickness of the boundary liquid film layer between the atmosphere and the main body of water. ZOX describes this film thickness. Increasing aeration flow rates should increase ZOX significantly. Because increased air flow rates cause larger air bubbles that exchange gas less efficiently, an increase in ZOX implies a slightly proportionally greater increase in the air flow rate (Wheaton, 1977, pp. 666 and 668). Figure 28 shows the effect of varying ZOX on fish growth. To make the variables in

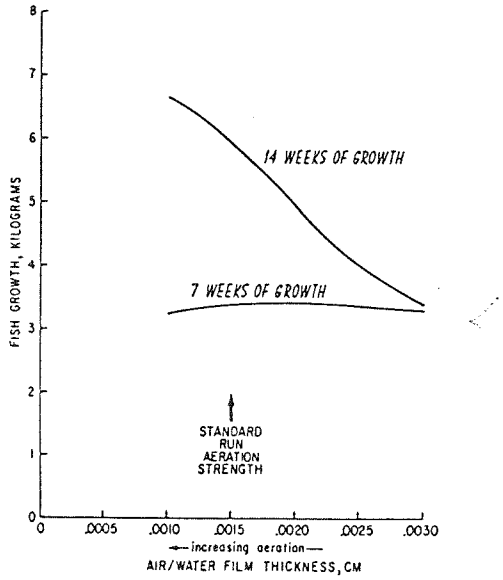

Fig. 28. Fish growth as a function of aeration.

this computer simulation "experiment" a bit steadier and consistent over time, we made a simplified version of the Pond H standard run. In the simplified version, the feeding rate is steady (FSW = 1) and the extraordinarily large draindowns are removed and kept at a steady 20% per week (EXCH1 = 0 & EXCH2 = 0).

It is readily apparent that the aeration strength is not critical for the first 7 weeks of growth, when oxygen is boosted by algal growth. On the other hand, during the second 7 weeks slight decreases in the aeration strength strongly affect fish growth. This makes some sense, since the algae have peaked and declined, and the ecosystem is dominated by bacterial and decomposition processes that create an oxygen deficit. If the aeration strength is halved (ZOX = 0.0030), fish growth during the second 7 weeks will decline to the point where it is negligible.

Sunlight algae

In the introduction, one of the stated purposes of the model was to explore the impact of algae on the fish culture ecosystem and fish growth. The model can easily simulate a shaded pond that will not allow the algae to survive. Table 6 compares a solar-algae pond with an equivalent darkened body of water under two feeding regimes, Pond H's standard run, and a more even feeding regime. The water exchange rate is a steady 20% per week.

In all cases the solar-algae pond slightly outperformed an equivalent shaded pond. The sunlight and algae had the greatest impact on ponds with uneven feeding rates (with a tendency for early un-ionized ammonia spikes). The greatest improvement in fish growth always occurred in the first 7-week period, when the algae was blooming. Algal growth appears beneficial, and

TABLE 6

Comparison of solar-algae ponds with shaded ponds under irregular (Pond H standard run) and even feeding regimes for 7- and 14-week durations

	Irregular feeding		Even feeding	
	Solar-algae	Shaded	Solar-algae	Shaded
Kilograms of fish growth:				
7 Weeks	2.31	2.05	3.37	3.32
14 Weeks	4.96	4.59	5.87	5.82
Percent improvement in growth, solar over shaded pond:				
7 Weeks	13%		2%	
14 Weeks	8%		1%	

the 'backlash' from the algal decline in the second 7-week period is not serious, and does not negate the initial advantage to fish growth.

Water exchange

Water draindowns replaced by fresh water remove not only soluble inorganic toxins such as ammonia and nitrite, but also organic particles that contain the potential to decompose and release these same toxins. This same decomposition also generates toxic carbon dioxide and depletes oxygen. These organic particles also shade the algae, diminishing the ability of the algae to photosynthesize and purify the water. Thus, one of the most effective methods of increasing fish growth is through increasing water exchange. The improvement is not linear, and instead exhibits steplike jumps. Figure 29 illustrates the impact of various water exchange rates on fish growth.

For Pond H's uneven feeding rate, a weekly exchange of 30% appears optimal for the first 7-week period, while the actual 20% exchange appears to be better for a steadier feeding rate. It is important to examine this initial 7-week period carefully, since it may be desirable to stop the run at this point, and restart with fresh water.

The total fish growth for the longer 14-week period displays a more complex curve. An initial optimum occurs at 20% per week; increasing to

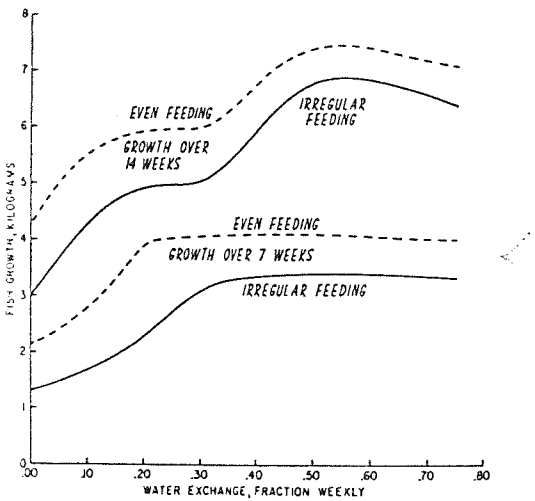

Fig. 29. Fish growth as a function of feeding eveness and water exchange.

30% yields virtually no increase in fish growth. Increasing the water exchange beyond 30% causes another rapid rise in fish growth, peaking at 50%. Increasing water exchange beyond 50% per week actually causes a decrease in fish growth. The first growth plateau (moving from 20 to 30% water exchange) results from removing too many heterotrophic bacteria, hindering the destruction of the shading organics and suppressing the final algae resurgence. The second growth plateau (beyond 50% water exchange) is linked to toxic un-ionized ammonia, the suppression of nitrifying bacteria that could oxidize the ammonia, and a paucity of microbial feeds for the fish. In front of these plateaus two optimum water exchange rates exist: 20 and 50% per week. If minor constraints on water supply are present, 20% appears optimal. Even this rate may be excessive in arid areas or in solar-heated greenhouses during the severest winter months when make-up water is quite cold. On the other hand, if warm supplemental water is abundant, the best fish growth occurs with a 50% weekly water exchange rate.

Particulate removal

In a series of hypothetical simulation runs, we postulated a very fine-sieved particulate filter, and examined various particulate removal rates. Such a filter would remove both suspended organic particulates and live algae. This series of experimental simulation runs showed that particulate removal alone yields nearly the same fish growth as a water exchange rate that removes the same fraction of particulates weekly. In fact, the results are so close (within a few percent), that we have not listed a comparison table here. Since the primary beneficial effect of water exchange is particulate removal, it becomes clear that much water can be conserved by concentrating the particulates into a smaller water volume before removal. This is accomplished by a secondary silo that acts as a settling tank. These 18-inch diameter tubes hold slightly more than 60 gal, or almost exactly 10% of the volume of a standard-sized solar-algae pond. The settling tank system has been developed and studied at New Alchemy; results are reported in Progress Report 4, pp. 29–36. The critical parameter of such a settling tank is the particulate concentration factor. Empirical evidence gathered by David Engstrom suggests the concentration factor varies from 3 to 4. Let us assume an organic concentration factor of 3, and an algae concentration factor of 2 (algae have less tendency to settle than nonliving organic particles). The model suggests that a system with a settling tank drained once weekly (10% of solar-algae pond volume) can yield nearly as much fish growth as draining the main pond 20% weekly. Although these simulation runs do not match the parameters for particular experiments reported, the general principles revealed by

the simulations are verified by the settling tank experiments. The water conservation benefits of auxiliary settling tanks are therefore evident. The ultimate extension of this approach would be to develop a particulate filter (essentially a 10–20 μm sieve). The computer model suggests that while removing virtually no water, such a filter could still maintain water purity.

SUMMARY

Researchers at the New Alchemy Institute thoroughly monitored over a 100-day experimental period the water chemistry and biological parameters of a unique aquaculture system, the solar-algae pond. The ponds are cilindrical containers, 1.5 m in diameter and height, with light transmitting walls, in which the blue tilapia, *Oreochromis aureus*, is grown. The computer model described herein accurately simulates the carbon, oxygen and nitrogen flows in this intensive fish culture system, as well as the accumulation of algae, bacteria and fish biomass. The modelling method, System Dynamics, and computer language, DYNAMO, were used to numerically solve the nonlinear differential equations describing this ecosystem. After successfully reproducing the observed data for three experimental runs for the aquaculture system, the model tested various management and design changes that might improve fish growth, including feeding strategies, aeration, water exchange, and a hypothetical 10 μm particulate filter. These simulation runs suggest that different management strategies are implied depending upon the length of the growing period. Up to the 7-week mark, the ponds experience relatively good water quality, while beyond this point the aquaculture system is dominated by organic decomposition and attendant loss of water quality. The model suggests that for a 7-week growth trial, an aeration coefficient of 0.2/h (film thickness of 0.003 cm) is sufficient, whereas for a 14-week trial a much stronger aeration coefficient of 0.6/h (film thickness of 0.001) is needed for greatest fish growth. Likewise, a water exchange rate of 20% per week attains optimal fish growth over a 7-week trial, while a 50% weekly water replacement rate is required for maximum fish yields over a 14-week period. Thus, the shift from an ecosystem emphasizing algal growth implies different management strategies.

The model also clarifies the role of the algae in this unique ecosystem. During the first 7 weeks, the model shows the algae contributed a small but significant improvement in the water quality and fish growth (a 2 to 13% increase in fish growth over a non-algal pond, depending upon feeding regime), while in the second 7-week period the influence of the algae was far outweighed by bacterial decomposition.

One of the most important aspects of this simulation model is the

inclusion of functually differentiated bacterial sectors. For instance, it is the *delay* between the establishment of decomposing/deaminating bacteria (that generate ammonia), and the growth of the nitrifying bacteria (that oxidize ammonia), that creates the ammonia spike commonly occurring in many aquaculture systems. Bacterial dynamics also present tremendous problems and challenges to aquacultural simulation modellers. Bacterial populations are very difficult to differentiate and empirically measure, often forcing investigators to infer the population dynamics from observed water chemistry fluctuations. As well, the kinetics of bacterial populations are extremely rapid (on the order of hours) relative to the time horizon of the fish growth trials (on the order of months). While the authors believe the dynamics of the decomposing and ammonia-oxidizing bacteria were successfully portrayed, the kinetics of the nitrite-oxidizing, nitrite-reducing and nitrate-reducing bacteria were so rapid that they could not be simulated satisfactorily. Spikes of nitrite and nitrate observed at the end of the experimental period (a highly eutrophic condition) were so frequent that every-other-day empirical measurements could not capture the shape and precise nature of these fluctuations.

One of the greatest strengths of comprehensive simulation models is to reveal areas where more basic research is required. We list a few areas:

(1) the role of microbial populations in the nutrition of tilapia fed exogenous feeds;

(2) the atmospheric/aquatic exchange of carbon dioxide, especially under an aeration regime;

(3) the mortality rate (senescence and lysing) of different functional bacterial groups under various conditions;

(4) the presence and role of organic compounds in inhibiting fish growth.

The last question is perhaps the most intriguing. Because of subtle discrepancies between occurrence of known inorganic fish toxins and reduced fish growth, the question arises whether inorganic compounds (e.g. CO_2, NH_3, NO_2^-, O_2) are the only relevant parameters in assessing water quality. The 'observed' toxicity of ionized ammonia, NH_4^+, may instead largely correlate with the presence of toxic organic compounds. It is possible that organic compounds produced by natural decomposition are playing a greater role than previously suspected.

The aquaculture simulation model described has great potential and usefulness. It suggests improved management strategies, and furthers fish culturists' understanding of the criticle dynamics in aquaculture systems, varying from indoor to outdoor ponds, and from flow-through to closed systems. A full explanatory documentation of the model, titled 'Assessment of a semi-closed, renewable, resource-based aquaculture system', Progress Report 6, Part II. Computer Simulation Model (171 pp.) is available for

US$25.00 from the New Alchemy Institute, 237 Hatchville Road, East Falmouth, Ma 02536, U.S.A.

ACKNOWLEDGEMENTS

This paper is dedicated to our many coworkers, whose careful and conscientious collection of data made this analysis possible. We feel a special indebtedness to the volunteers who selflessly contributed many hours, weeks and months of their talented time to the project. They include: Alex Barnum, Daryl Bergquist, Leonore Botero, Peter Burgoon, Terry Butler, Cathy Cetta, Barbara Chase, Chris Copeland, Roland DuBois, Dick Earles, Laurie Fulton, Donna Goldberg, Carl Goldfisher, Deborah Goodwin, Michael Greene, Linda Gusman, Elizabeth Hasslacher, Tom Heggestad, Bill Hough, Kaaren Janssen, David Juers, Darcy King, Lisa Lystad, Meredith Olsen, Tula Quast, Nancy Russell, Sherry Sass, Paul Silverstein, Ken Winnick, Nancy Wright, and Josh Zimmerberg.

Deep thanks must be given to fellow staff on the solar aquaculture research team: Carl Baum, Daryl Bergquist, Al Doolittle and Kathleen Whitacre. Drs. John Todd and William McLarney founded New Alchemy Institute's aquaculture program, upon which this research was based. As co-principle investigator, John Todd provided inspiring leadership and wise guidance throughout the project's history.

We would like to extend special appreciation to Drs. Donella and Dennis Meadows, who offered encouragement and invaluable support at every stage of the model's development.

Finally, we would like to thank the National Science Foundation Program Directors who oversaw our project: Drs. Lynn Preston and Ed Bryan. Their roles in the Appropriate Technology Program made this and many other crucial research endeavors possible.

REFERENCES

Almazan, G. and Boyd, C.E., 1978. Plankton production and tilapia yield in ponds. Aquaculture, 15: 75–77.

Arce, R. and Boyd, C.E., 1975. Effects of agricultural limestone on water chemistry, phytoplankton productivity and fish production in soft water ponds. Trans. Am. Fish. Soc., 104: 308–312.

Behrens, J.C., Beyer, J.A., Madsen, O.B.G. and Thomsen, P.G., 1975. Some aspects of modelling the long-term behaviour of aquatic ecosystems. Ecol. Modelling, 1: 163–198.

Bodansky, O., 1951. Methemoglobin and methemoglobin-producing compounds. Pharm., Rev., 3: 144–196.

Brewer, P.G. and Goldman, J.C., 1976. Alkalinity changes generated by phytoplankton growth. Limnol. Oceanogr., 21(1): 108–117.

Brock, Th.D., 1979. Biology of Microorganisms. Prentice-Hall, Inc., Englewood Cliffs, NJ, 3rd edn.

Broeker, W.S., 1974. Chemical Oceanography. Harcourt, Brace and Jovanovich.

Brooks, J.L. and Dodson, S.I., 1965. Predation, body size and composition of plankton. Science, 150: 28–35.

Collins, M.T. et al., 1975. Nitrification in an aquatic recirculating system. J. Fish. Res. Board Can., 32: 2025–2031.

Crawford, R.E. and Allen, G.H., 1977. Seawater inhibition of nitrite toxicity to chinook salmon. Trans. Am. Fish. Soc., 106(1): 105–109.

Davisson, W.I. and Uhran, J.J., 1977. A Primer for NDTRAN: A Dystem Dynamics Interpreter. University of Notre Dame, Notre Dame, IN, 244 pp.

Duffie, J.A. and Beckman, W.A., 1974. Solar energy Thermal Processes. John Wiley & Sons, New York, NY, 386 pp.

Duffie, J.A. and Beckman, W.A., 1980. Solar Engineering of Thermal Processes. John Wiley & Sons, New York, NY, 762 pp.

Forrester, J.W., 1968a. Principles of Systems. Wright-Allen Press, Cambridge, MA, 391 pp.

Forrester, J.W., 1968b. Industrial Dynamics The M.I.T. Press, Cambridge, MA.

Forrester, J.W., 1973. World Dynamics. Wright-Allen Press, Cambridge, MA, 144 pp.

Forrester, N.B., 1969. A computer approach to environmental system design—dynamics of a predator–prey relationship. In house paper available from the author, M.I.T.

Goodman, M.R., 1974. Study Notes in System Dynamics. Wright-Allen Press, Cambridge, MA, 388 pp.

Hutchinson, G.E., 1957. A Treatise on Limnology. Vol. I: Geography, Physics and Chemistry. John Wiley & Sons, New York, NY, 1015 pp.

Jørgrnsen, S.E., Mejer, H. and Friis, M., 1978. Examination of a lake model. Ecol. Modelling, 4: 253–278.

Koch, Ph.D.L., 1975. DTSS Dynamo Reference Manual. TM043. Kiewitt Computation Center, Hanover, NH, 89 pp.

May, R.M., 1975. Stability and Complexity in Model Ecosystems. Princeton University Press, Princeton, NJ.

May, R.M., 1976. Models for single populations, and Models for two interacting populations. In: R.M. May (Editor), Theoretical Ecology: Principles and Applications. W.B. Saunders Company, Philadelphia, PA, Chapters 2 and 4, pp. 4–25 and 49–70.

McConnell, W.J., 1965. Relationship of herbivore [*Tilapia mossambique*] growth to rate of gross photosynthesis in microcosms. Limnol. Oceanogr., 10: 539–543.

Meadows, D.H. et al., 1972. The limits to Growth. Universe Books, New York, NY.

Meadows, D.L. et al., 1974. The Dynamics of Growth in a Finite World. Wright-Allen Press, Cambridge, MA, 637 pp.

Murphy, T.P., Lean, D.R.S. and Nalewajko, C., 1976. Blue-green algae: their excretion of iron-selective chelators enables them to dominate other algae. Science, 192: 900–902.

New Alchemy Institute Solar Aquaculture Research Staff. Assessment of a semi-closed renewable resource-based aquaculture system. The National Science Foundation Project No. OPA 77-16790 A01. Progress Reports I, 3, 4, and 5 are available from the National Technical Information Service, U.S. Dep. of Commerce, Springfield, VA 22161.

Progress Report 1, 1978a. Angevine, Doolittle, Engstrom, Olson, Todd, Wolfe and Zweig. ("A Six-Month Progress Report, May 23, 1978"). 88 pp. NTIS No. PB287286/AS.

Progress Report 2, 1978b. Angevine, Doolittle, Engstrom, Todd, Wolfe, Zweig, Butler, Goodwin and Janssen. ("Interim Report, August 24, 1978"). 31 pp.

Progress Report 3, 1979a. Angevine, Doolittle, Engstrom, Todd, Wolfe and Zweig. 128 pp.

Progress Report 4, 1979b. Angevine, Doolittle, Engstrom, Todd, Wolfe and Zweig. 71 pp. NTIS No. PB80-105471.

Progress Report 6, Part 2. Wolfe. NTIS No. PB81-143166.

Payne, R.E., 1977–1981. Monthly Climatological Sheets. Woods Hole Oceanographic Institute, Woods Hole, MA.

Perrone, S.J. and Meade, T.L., 1977. Protective effect of chloride on nitrite toxicity to coho salmon (*Onchorhynchus ritsutch*). J. Fish. Res. Board Can., 34(4): 486–492.

Pieri, R.V. and Converse, A.O., 1974. A dynamic model for lake water quality management. Thayer School of Engineering, Hanover, NH.

Pugh, L. III, 1977. DYNAMO User's Manual. The M.I.T. Press, Cambridge, MA, 131 pp.

Shaffer, W.A., 1977. Installing Mini-DYNAMO. Pugh-Roberts Associates, Cambridge, MA, 38 pp.

Shaffer, W.A., 1978. Mini-DYNAMO User's Guide. Pugh-Roberts Associates, Cambridge, MA, 67 pp.

Sharma, B. and Ahlert, R.C., 1977. Nitrification and nitrogen removal. Water Res., 11: 897–925.

Stumm, W. and Morgan, J.J., 1970. Aquatic Chemistry. John Wiley and Sons, New York, NY, 593 pp.

Wetzel, R.G., 1975. Limnology. W.B. Saunders Co., Philadelphia, PA, 743 pp.

Wheaton, F.W., 1977. Aquacultural Engineering. John Wiley & Sons, New York, NY, 708 pp.

Wolfe, J., Engstrom, D. and Zweig, R., 1980. Sunlight patterns without, chemistry patterns within: the view from a solar-algae pond. J. New Alchemists, 6: 100–106.

Wolfe, J., Engstrom, D. and Zweig, R., 1981. Modelling algal growth and decline in solar-algae ponds. J. New Alchemists, 7: 88–94.

Yanling, L., Melack, J.M. and Ji, W., 1981. Primary production and fish yields in Chinese ponds and lakes. Trans. Am. Fish. Soc., 110: 346–350.

Young, T.B., Bruley, D.F. and Bungay III, H.R., 1970. A dynamical model mathematical model of the chemostat. Biotech. Bioeng., 12: 747–769.

Zweig, R.D., 1977. The sage of the solar-algae ponds. J. New Alchemists, 4: 63–68.

Zweig, R., Wolfe, J., Engstrom, D. and Doolittle, A., 1981. Solar aquaculture: an ecological approach in human food production. In: L.J. Allen and E.C. Kinney (Editors), Proceedings of the Bio-engineering Symposium for Fish Culture. Fish Culture Section of the American Fisheries Society, Bethesda, MD, pp. 210–226.

APPENDIX

***ANNOTATED LISTING: ECOSYSTEM MODEL OF SOLAR-ALGAE POND H, AUG-NOV 1978**

VARIABLE NAMES		DYNAMO EQUATIONS		
	100	*		SOLAR-ALGAE POND H, AUG-NOV 1978.
	110	NOTE		
	120	NOTE		FISH SECTOR
	130	NOTE		
FISH BIOMASS, gm wet wt	140	L		FISH.K=FISH.J+(DT)(FISHGRO.JK)
FISH BIOMASS INITIALLY	150	N		FISH=FISHI
FISH BIOMASS INIT., gmwet	160	C		FISHI=2010
FISH POPULATION, tilapia	170	C		FPOP=46
AVERAGE FISH SIZE, gmwet	180	A		SIZE.K=FISH.K/FPOP
	190	NOTE		

FISH GROWTH, gmwet/day	200	R	FISGRO.KL=FASSM.K-FRESP.K
FISH ASSIMILATION, gmwet/day	210	A	FASSM.K=ASSM.K*WETR*(EFEED.K*LNGF+
(Line Continuation)	220	X	BAFI.K/BACNC+ALFI.K/ALGNC)
BACTERIA FISH INGESTION Rate	230	A	BAFI.K=BAC1FD.K+BAC2FD.K+BAC3FD.K+
gm Nitrogen/day (gmN/day)	235	X	BAC4FD.K+BAC5FD.K
LOW NITROGEN GROWTH FACTOR	240	C	LNGF=1
less than 1 for low N feeds			
BACTERIA NITROGEN CONTENT	250	C	BACNC=.09
gm N/ gm dry weight			
ALGAE N CONTENT (gmN/gmdry)	260	C	ALGNC=.09
ASSIMILATED FRACTION OF	270	A	ASSIM.K=ASSF.K*MAXAS
INGESTED FEED **			
WET-TO-DRY WEIGHT RATIO	280	C	WETR=4.0
fish biomass; gmwet/gmdry			
MAX. ASSIMILATION EFFICIENCY	290	C	MAXAS=.31
EATEN FEED, gmdw/day	300	A	EFEED.K=MIN(FEED.K,SAT.K)
SATIATION LIMIT, gmdw feed/d	310	A	SAT.K=FISH.K*MAXSAT*TOXSF.K*SIZEF.K
FISH SIZE FACTOR	320	A	SIZEF.K=(SIZE.K/100) SIZEFC
FISH SIZE FACTOR COEFFICIENT	330	C	SIZEFC=-.20
MAX. SATIATION COEFFICIENT	340	A	MAXSAT=.042
dw feed/ ww fish			
FOOD CONVERSION RATIO,	350	A	FCRI.K=MAX(FEED.K,.01)/
INSTANTANEOUS, dwfeed/wwfish	355	X	MAX((FASSM.K-FRESP.K),.01)
FOOD CONVERSION RATIO,	360	A	FCRA.K=FED.K/MAX(GROWTH.K,.1)
CUMULATIVE, dw feed/ww fish			
CUMULATIVE FISH GROWTH, gmww	370	A	GROWTH.K=FISH.K-FISHI
CUM. GROWTH RATE, gmww/day	380	A	GRORAT.K=GROWTH.K/MAX(TIME.K,.1)
FISH RESPIRATION, gmww/day	390	A	FRESP.K=FISH.K*FRESC*SIZEF.K
FISH RESP. COEF., per day	400	C	FRESC=.01
UNASSIMILATED FEED, gmdw/day	410	A	UNAS.K=EFEED.K*(1-ASSIM.K)
UNEATEN FEED, gmdw/day	420	A	UNEAT.K=MAX(0,FEED.K-SAT.K)
ORGANIC INPUT FROM FEED	430	A	ORGIN.K=UNAS.K+UNEAT.K
gmdw/day	440	NOTE	
ASSIMILATION FACTOR	450	A	ASSF.K=TABHL(ASSFT,TOXIN.K,0,10,1)
reduces fish assim. of feed			
at high toxicity levels			
TABLE, ASSIM. FACTOR ***	460	T	ASSFT=1.0/.92/.9/.8/.6/
function of toxicity index	465	X	.4/.3/.2/.1/.05/.02
TOXICITY SATIATION FACTOR	470	A	TOXSF.K=CLIP(TSF.K,0,TSF.K,0)
lowers fish appetite at	480	A	TSF.K=MTOX*TOXIN.K+BTOX
high toxicity levels	490	C	MTOX=-.06
MTOX & BTOX are the slope &	500	C	BTOX=1.0
y-intercept of the function			
TOXICITY INDEX	510	A	TOXIN.K=DOXTOX.K+AMMTOX.K+NH3TOX.K
			+NO2TOX.K+CO2TOX.K
DEPLETION-OF-OXYGEN TOXICITY	520	A	DOXTOX.K=DOXTX*(1.2-OXF.K)
TOTAL AMMONIA TOXICITY	530	A	AMMTOX.K=AMMTX*AMM.K
UN-IONIZED AMMONIA TOXICITY	540	A	NH3TOX.K=NH3TX*NH3.K
NITRITE, NO2-, TOXICITY	550	A	NO2TOX.K=NO2TX*NO2.K
CARBON DIOXIDE, CO2, TOXICTY	560	A	CO2TOX.K=CO2TX*CO2.K
ANOXIA TOXICITY COEFICIENT	570	C	DOXTX=4.0
per gm O/pond			
TOTAL AMMONIA TOXICITY COEF.	580	C	AMMTX=.08
per gm N/pond			
UN-IONIZED AMMONIA TOX.COEF.	590	C	NH3TX=4.0
per gm N/pond			

```
NITRITE TOXICITY COEFICIENT  600 C     NO2TX=.05
 per gm N/pond
CARBON DIOXIDE TOX. COEF.    610  C    CO2TX=.12
 per gm CO2/pond
                             620  NOTE
                             630  NOTE EXOGENOUS VARIABLES SECTOR
                             640  NOTE
AMOUNT FED TO POND, gmdw     650  L    FED.K=FED.J+(DT)(FEDIN.JK)
INITIAL AMOUNT FED, gmdw     660  N    FED=0
FED INPUT,    gmdw/day       670  R    FEDIN.KL=FEED.K
FEEDING RATE, gmdw/day       680  A    FEED.K=DRYR*SWITCH(FEED1.K,FEED2.K,FSW)
 switch: FSW=0 gives daily
 feed schedule, FEED1; FSW=1
 gives biweekly sched, FEED2
DRY-TO-WET FEED RATIO        690  C    DRYR=.92
 pelleted feed is 92% dry
FEEDING SWITCH (see 680)     700  C    FSW=0
ACTUAL FEEDING SCHEDULE      710  A    FEED1.K=TABHL(FEED1T,TIME.K,0,100,1)
 gm feed/day                 720  T    FEED1T=120/120/060/120/120/120/000/
                             730  X          120/142/142/142/142/142/000/
                             740  X          180/180/180/180/000/000/000/
                             750  X          000/000/000/000/000/210/000/
                             760  X          000/374/230/230/230/230/000/
                             770  X          270/270/270/270/270/000/000/
                             780  X          148/148/000/148/148/148/000/
                             790  X          175/178/000/178/000/178/000/
                             800  X          210/210/210/210/210/210/000/
                             810  X          248/248/000/248/248/000/000/
                             820  X          248/000/150/150/150/000/000/
                             830  X          150/150/150/000/150/150/000/
                             840  X          150/150/150/150/150/150/000/
                             850  X          150/150/150/150/150/150/000/
                             860  X          150/150/150
AVERAGED FEEDING SCHEDULE    870  A    FEED2T.K=TABHL(FEED2T,TIME.K,0,98,14)
 more even and continuous    880  T    FEED2T=101/111/107/149/141/121/118/124
                             890  NOTE
SUNLIGHT ENTERING WATER      900  A    SUN.K=TABHL(SUNT,TIME.K,0,100,1)
 (million calories/day)      910  T    SUNT=14.0/05.2/06.4/12.9/14.5/10.4/15.4
 This table is derived from  920  X        /09.6/16.2/19.2/18.5/21.8/11.6/16.3
 daily total solar radiation 930  X        /21.0/21.2/16.7/12.2/22.2/22.5/14.5
 on a horizontal surface,    940  X        /18.0/21.1/21.5/10.2/03.2/15.4/21.6
 and then analyzed using a   950  X        /08.5/16.4/18.8/06.9/12.1/21.5/21.3
 secondary computer model    960  X        /15.8/22.0/20.7/12.1/13.8/17.9/17.5
 that predicts direct, dif-  970  X        /07.3/10.5/17.4/18.1/09.7/20.7/18.1
 fuse & reflected sunlight   980  X        /04.3/15.7/18.4/16.8/07.5/10.5/17.6
 on all surfaces of the pond 990  X        /16.4/18.8/13.6/13.1/17.5/18.4/13.2
 cylinder, the associated    1000 X        /16.9/09.8/06.2/14.4/06.7/15.7/15.9
 angles of incidence (and    1010 X        /19.1/16.6/15.9/15.6/14.2/03.8/06.6
 thus the fraction of light  1020 X        /17.3/15.6/17.8/10.5/06.8/15.0/15.1
 transmitted), and finally,  1030 X        /15.5/13.0/07.3/15.5/16.0/16.1/14.9
 total sunlight penetrating  1040 X        /12.0/11.6/15.4/17.0/09.0/08.0/10.7
 into the water column.      1050 X        /11.8/02.8/16.4
                             1060 NOTE
WATER OUTFLOW SCHEDULE       1070 A    OUT.K=SWITCH(OUT1.K,OUT2,OSW)
 fraction H2O per day
OUTFLOW SWITCH               1080 C    OSW=0
```



```
ACTUAL OUTFLOW/REPLACEMENT   1090 A    OUT1.K=PULSE(EXCH/DT,FRST,INVL)
 (fraction H20 per day)      1100 X          +PULSE(EXCH1/DT,FRST1,INVL1)
 20% drain downs and water   1110 X          +PULSE(EXCH2/DT,FRST2,INVL2)
 replacement occurred each   1120 C    EXCH=.20
 week; exceptions: 66% on    1130 C    FRST=8
 17th day and 50% on 64th    1140 C    INVL=7
 day.                        1150 C    EXCH1=.46
                             1160 C    FRST1=17
                             1170 C    INVL1=200
                             1180 C    EXCH2=.30
                             1190 C    FRST2=64
                             1200 C    INVL2=200
OUTFLOW REGIME # 2           1210 C    OUT2=.025
 fraction H2O per day
 .025/day = .2/week, and
 thus can test effect of
 even, continuous drains
PARTICULATE FILTRATION       1220 C    FILT=0
 fraction of org & algae/day
 This can test a hypothetical
 particulate filter
ACCUMULATED OUTFLOW TOTAL    1230 L    OUTOT.K=OUTOT.J+(DT)(OUTFLOW.JK)
 cumulative volumes of H2O   1240 N    OUTOT=0
 exchanged; only an indica-  1250 R    OUTFLO.KL=OUT.K
 tor variable.
                             1255 NOTE AERATION: SEE ZAM, EQNS. 1980-2010
                             1256 NOTE           AND ZOX, EQNS. 2490-2510
                             1260 NOTE
                             1270 NOTE ALGAE SECTOR
                             1280 NOTE
ALGAE BIOMASS                1290 L    ALG.K=ALG.J+(DT)(NITALG.JK-ALGORG.JK
 grams Algal Nitrogen/Pond   1300 X         -ALGOUT.JK-ALGFIS.JK)
ALGAE BIOMASS INITIALLY      1310 N    ALG=ALGI
 gm N/pond                   1320 C    ALGI=1.0
                             1330 NOTE
NITROGEN-TO-ALGAE RATE.KL    1340 R    NITALG.KL=NITAG.K
 gm N/pond*day  ****
 (algae growth rate)
NITROGEN-TO-ALGAE RATE.K     1350 A    NITAG.K=ALG.K*(MAXAG.K*SUNF.K-ARES)
ALGAE RESPIRATION, per day   1360 C    ARES=.15
MAXIMUM ALGAL GROWTH, SPECI- 1370 A    MAXAG.K=MAXAGC*TABHL(MAXAGT,NTOT.K/CF,
 FIC RATE (per day)          1375 X                              0,4,1)
TABLE, MAX. ALGAL GROWTH     1380 T    MAXAGT=0/.7/.9/1/1
MAX ALGAL GROWTH COEFFICIENT 1390 C    MAXAGC=.7
NITROGEN TOTAL, soluble      1400 A    NTOT.K=AMM.K+NO3.K
 inorganic gm N/pond
SUNLIGHT FACTOR              1410 A    SUNF.K=SUN.K*(SUNC/SUNREF)
 Note: EXP(-X) = e^-X        1415 X          *(EXP(-SHADEF.K))
SUNLIGHT CONSTANT            1420 C    SUNC=1
SUNLIGHT REFERENCE LEVEL     1430 C    SUNREF=12
 million calories/day
SHADING FACTOR               1440 A    SHADEF.K=(ALG.K+ORG.K*OSHAD)/SHADEC
SHADE COEFFICIENT gm N/pond  1450 C    SHADEC=125
ORGANICS SHADING FACTOR      1460 C    OSHAD=1
ALGAE-TO-ORGANICS RATE       1470 R    ALGORG.KL=ALG.K*ALGDC
 gm N/pond*day  (algae
```

```
ALGAE DEATH COEF., per day      1480 C    ALGDC=.08
ALGAE-TO-FISH RATE.KL           1490 R    ALGFIS.KL=ALFI.K
ALGAE-TO-FISH RATE.K            1500 A    ALFI.K=ALG.K*ALAF.K*TOXSF.K
 gm N/pond*day                                    *FRESP.K/FRI.K
 (fish predation on algae)
ALGAE ASSIMILATION FACTOR       1510 A    ALAF.K=TABHL(ALAFT,TIME.K,0,30,15)
 After the first 30 days        1520 T    ALAFT=.25/.20/.02
 most algae are small and
 thick-walled, evading the
 heavy predation pressure.
FISH RESPIRATION INITIALLY      1530 A    FRI.K=FISHI*FRESC
 gm wet fish/day.  Analogous                    *((FISHI/(FPOP*100)) SIZEFC)
 to FRESP.K, see line 390.
ALGAE OUTFLOW RATE              1540 R    ALGOUT.KL=ALG.K*(AOF.K+FILT)
 gm N/pond*day
ALGAE OUTFLOW FACTOR, /day      1550 A    AOF.K=SWITCH(AOF1.K,OUT.K,OSW)
ALGAE OUTFLOW FACTOR 1, /day    1560 A    AOF1.K=CLIP(AOF11.K,AOF12.K
 The amount of water removed    1570 A                ,OUT.K,OUTREF)
 in a drain-down determines     1580 X    AOF11.K=OUTREF*AOCF+((OUT-OUTREF)
 whether water is drawn only    1590 A              *(1-OUTREF*AOCF)/(1-OUTREF))
 from the concentrated lower             AOF12.K=OUT.K*AOCF
 reaches of the pond, or
 extends up into more dilute
 regions.
ALGAE OUTFLOW CONC. FACTOR      1600 C    AOCF=1
 Ratio: algae concentration
 in OUTREF/ av. algae conc.
 If AOCF=1, algae is evenly
 dispersed through top and
 bottom regions of the pond.
OUTFLOW REFERENCE FRACTION      1610 C    OUTREF=.1
 A reference BOTTOM region
                                1620 NOTE
                                1630 NOTE SUSPENDED ORGANIC PARTICLES
                                1640 NOTE
SUSPENDED ORGANIC PARTICLES     1650 L    ORG.K=ORG.J+(DT)(FEDORG.JK+ALGORG.JK
 gm N/pond                      1655 X          -ORGAMM.JK-ORGOUT.JK)
ORGANICS INITIALLY              1660 N    ORG=ORGI
 gm N/pond                      1670 C    ORGI=0
FEED WASTES-TO-ORGANICS         1680 R    FEDORG.KL=ORGIN.K*FEDNC
 gm N/pond*day
FEED NITROGEN CONTENT           1700 C    FEDNC=.078
 gm N/ gm dry weight
ORGANICS-TO-AMMONIA             1710 R    ORGAMM.KL=OGAM.K
 gm N/pond*day; a.k.a the       1720 A    OGAM.K=ORG.K*BAC1.K*OGAMC*OXF.K
 organic decomposition rate
ORGANICS-TO-AMMONIA COEF.       1730 C    OGAMC=.02
 day^-1 gm N^-1
ORGANICS OUTFLOW RATE           1740 R    ORGOUT.KL=ORG.K*(OOF.K+FILT)
 gm N/pond*day
ORGANICS OUTFLOW FACTOR         1750 A    OOF.K=SWITCH(OOF1.K,OUT.K,OSW)
 per day; analogous to AOF,     1760 A    OOF1.K=CLIP(OOF11.K,OOF12.K
 see lines 1550 - 1610                            ,OUT.K,OUTREF)
                                1770 A    OOF11.K=OUTREF*OOCF+((OUT.K-OUTREF)
                                1780 X          *(1-OUTREF*OOCF)/(1-OUTREF)
                                1790 A    OOF12.K=OUT.K*OOCF
```



```
ORGANIC OUTFLOW CONC, FACT.     1800 C    OOCF=1.2
 Organic particles do tend
 to be more concentrated
 toward the pond bottom.
                                1810 NOTE
                                1820 NOTE AMMONIA (NH3,NH4+) SECTOR
                                1830 NOTE
TOTAL AMMONIA, gm N/pond        1840 L    AMM.K=AMM.J+(DT)(ORGAMM.JK+FISAMM.JK
                                1850 X    -AMMALG.JK-NH3AIR.JK-AMMNO2.JK-AMMOUT.JK
AMMONIA INITIALLY               1860 N    AMM=AMMI
 gm N/pond                      1870 C    AMMI=.001
AMMONIA CONCENTRATION           1880 A    AMMMCON.K=AMM.K/CF
 mg N/liter
CONCENTRATION FACTOR            1890 C    CF=2.3
 2300 liters/pond *
 1 gm / 1000 mg
                                1900 NOTE
FISH-TO-AMMONIA RATE            1910 R    FISAMM.KL=FSAM.K
 gm N/pond*day; ammonia gen-    1920 A    FSAM.K=FRESP.K*FISNC
 erated by fish respiration
FISH NITROGEN CONTENT           1930 C    FISNC=.038
 nitrogen/ wet weight, from
 Caulton and Bursell, 1977.
AMMONIA-TO-ALGAE RATE           1940 R    AMMALG.KL=NITAG.K*AMM.K/NTOT.K
 gm N/pond*day; ammonia
 assimilation by algae
UN-IONIZED (TOXIC) AMMONIA      1950 A    NH3.K=NH3F.K*AMM.K
 gm N/pond
UN-IONIZED AMMONIA FRACTION     1960 A    NH3F.K=TABHL(NH3FT,PH.K,5,9,.5)
 Fraction of NH3 to total       1970 T    NH3FT=0/.0002/.0006/.002/.006
 ammonia is a highly non-       1975 X          /.018/.054/.153/.362
 linear function of pH.
NH3-TO-AIR RATE                 1980 R    NH3AIR.KL=DNH3*NH3.K/(DEPTH*ZAM)
 gm N/pond*day
DIFFUSION COEF. FOR NH3         1990 C    DNH3=2.76
 cm^2/day, from Broeker, 1974
POND DEPTH, cm                  2000 C    DEPTH=145
AIR/WATER Z-FILM THICKNESS      2010 C    ZAM=.03
 FOR AMMONIA, cm *****
 daytime, nonaeration z-film
AMMONIA-TO-NITRITE RATE         2020 R    AMMNO2.KL=AMNO2.K
 (NITRIFICATION STEP ONE)       2030 A    AMNO2.K=BAC2.K*AMM.K*AMNO2C*OXF.K
 gm N/pond*day
AMMONIA-TO-NITRITE COEF.        2040 C    AMNO2C=.2
 gm N^-1 day^-1
AMMONIA OUTFLOW RATE            2050 R    AMMOUT.KL=AMM.K*OUT.K
 gm N/ pond*day
                                2060 NOTE
                                2070 NOTE NITRITE (NO2-) SECTOR
                                2080 NOTE
NITRITE, NO2-                   2090 L    NO2.K=NO2.J+(DT)(AMMNO2.JK-NO2NO3.JK
 gm N/pond                      2100 X          +NO3NO2.JK-NO2N2.JK-NO2OUT.JK)
NITRITE, INITIALLY              2110 N    NO2=NO2I
 gm N/pond                      2120 C    NO2I=0
NITRITE CONCENTRATION           2130 A    NO2CON.K=NO2.K/CF
 mg N/liter                     2140 NOTE
```

```
NITRITE-TO-NITRATE RATE          2150 R    NO2NO3.KL=NIT23.K
 (NITRIFICATION STEP TWO)        2160 A    NIT23.K=BAC3.K*NO2.K*NO2NO3C*OXF.K
 gm N/pond*day
NO2-TO-NO3 COEFFICIENT           2170 C    NO2NO3C=.7
 gm N^-1 day^-1
NITRATE-TO-NITRITE RATE          2180 R    NO3NO2.KL=NIT32.K
 (DENITRIFICATION STEP ONE)      2190 A    NIT32.K=BAC4.K*NO3.K*NO3NO2C*(NOXC-OXF.K
 gm N/pond*day
NO3-TO-NO2 COEFFICIENT           2200 C    NO3NO2C=.7
 gm N^-1 day^-1
ANOXIA COEFFICIENT               2210 C    NOXC=1.4
NITRITE-TO-NITROGEN RATE         2220 R    NO2N2.KL=DENIT.K
 (DENITRIFICATION STEP TWO)      2230 A    DENIT.K=BAC5.K*NO2.K*NO2N2C*(NOXC-OXF.K
 gm N/pond*day
NO2-TO-N2 COEFFICIENT            2240 C    NO2N2C=.6
 gm N^-1 day^-1
NITRITE OUTFLOW RATE             2250 R    NO2OUT.KL=NO2.K*OUT.K
 gm N/pond*day

                                 2260 NOTE
                                 2270 NOTE NITRATE (NO3-) SECTOR
                                 2280 NOTE
NITRATE, NO3-                    2290 L    NO3.K=NO3.J+(DT)(NO2NO3.JK-NO3NO2.JK
 gm N/pond                       2300 X          -NO3ALG.JK-NO3OUT.JK)
NITRATE, INITIALLY               2310 N    NO3=NO3I
 gm N/pond                       2320 C    NO3I=0
NITRATE CONCENTRATION            2330 A    NO3CON.K=NO3.K/CF
 mg N/liter                      2340 NOTE
NITRATE-TO-ALGAE RATE            2350 R    NO3ALG.KL=NITAG.K*NO3.K/NTOT.K
 gm N/pond*day; nitrate
 assimilation by algae
NITRATE OUTFLOW RATE             2360 R    NO3OUT.KLJ=NO3.K*OUT.K
 gm N/pond*day

                                 2370 NOTE
                                 2380 NOTE OXYGEN (O2) SECTOR
                                 2390 NOTE
OXYGEN, O2                       2400 L    OX.K=OX.J+(DT)(ALGOX.JK+AIROX.JK-OXORG.
 gm O/pond                       2410 X         -OXFIS.JK-OXAMM.JK-OXNO2.JK)
OXYGEN, INITIALLY, gm O/pond     2420 N    OX=OXSAT
OXYGEN SATURATION AT 25° C       2430 C    OXSAT=18.6
 gm O/pond; equals 8.1 mgO/l
 times conc. factor 2.3 (CF)
OXYGEN CONCENTRATION             2440 A    OXCON.K=OX.K/CF
                                 2450 NOTE
ALGAE OXYGENATION RATE           2460 R    ALGOX.KL=ALGO2.K
 gm O/pond*day; from photo-      2470 A    ALGO2.K=NITAG.K*AONR
 synthesis
ALGAE OXYGENATION/ NITROGEN      2480 C    AONR=7.25
 ASSIMILATION RATIO, gmO/gmN
 based on algae composition
 of C7H10O3N, Verhoff, 1972
AIR/WATER OXYGEN EXCHANGE        2490 R    AIROX.KL=DOX*(OXSAT-OX.K)/(DEPTH*ZOX)
 RATE, gm O/pond*day
DIFFUSION COEF. FOR OXYGEN       2500 C    DOX=2
 cm^2/day, Broeker, 1974
AIR/WATER Z-FILM THICKNESS       2510 C    ZOX=.0015
 FOR OXYGEN, cm; reflects
```



```
 nighttime aeration; see
 discussion *****
OXIDATION-OF-ORGANICS RATE       2520 R    OXORG.KL=O2ORG.K
 gm O/pond*day; oxygen lost      2530 A    O2ORG.K=OGAM.K*OONR
 by organic decompostion
ORGANICS OXYGEN/NITROGEN         2540 C    OONR=7.25
 RATIO, gm O/ gm N
OXYGEN-TO-FISH RATE, gm O/       2550 R    OXFIS.KL=O2FIS.K
 pond*day; oxygen consumed       2560 A    O2FIS.K=FRESP.K*FONR*FISNC
 through fish respiration
FISH OXYGEN/NITROGEN RATIO       2570 C    FONR=7.25
 gm O/ gm N
OXIDATION-OF-AMMONIA RATE        2580 R    OXAMM.KL=AMNO2.K*ONR12
 gm O/pond*day; oxygen lost
 in ammonia-to-nitrite conv.
OXYGEN/NITROGEN RATIO FOR        2590 C    ONR12=3.22
 AMM-TO-NO2 PROCESS, gmO/gmN
 Wezernak & Gannon, 1967.
OXIDATION-OF-NITRITE RATE        2600 R    OXNO2.KL=NIT23.K*ONR23
 gm O/pond*day
OXYGEN/NITROGEN RATIO FOR        2610 C    ONR23=1.11
 NO2-TO-NO3, gm O/ gm N,
 Wezernak & Gannon, 1967.
                                 2620 NOTE
OXYGEN FACTOR                    2630 A    OXF.K=TABHL(OXFT,OXCON.K,0,6,1)
 influences the rate of all      2640 T    OXFT=0/.5/.8/.9/1.0/1.1/1.2
 aerobic processes based on
 the dissolved oxygen conc.
                                 2650 NOTE
                                 2660 NOTE CARBON DIOXIDE (CO2) SECTOR
                                 2670 NOTE
CARBON DIOXIDE, CO2              2680 L    CO2.K=CO2.J+(DT)(FISCO2.JK+ORGCO2.JK
 gm CO2/pond                     2690 X         +AIRCO2.JK-CO2ALG.JK)
CARBON DIOXIDE, INITIALLY        2700 N    CO2=CO2SAT
CARBON DIOXIDE SATURATION        2710 C    CO2SAT=1.15
 gm CO2/pond; .5 mg CO2/ltr
 times CF (=2.3); Hutchinson,
 1957, and Skirrow, 1965.
CARBON DIOXIDE CONCENTRATION     2720 A    CO2CON.K=CO2.K/CF
 mg CO2/ liter
                                 2730 NOTE
CARBON DIOXIDE/ OXYGEN RATIO     2740 C    COR=1.33
 gm CO2 /gm O2; based on
 stochiometry C7H10O3N
FISH-TO-CARBON DIOXIDE RATE      2750 R    FISCO2.KL=O2FIS.K*COR
 gm CO2/pond*day; CO2 from
 fish respiration
ORGANICS-TO-CO2 RATE             2760 R    ORGCO2.KL=O2ORG.K*COR
 gm CO2/pond*day; CO2 from
 organic decompostion
CO2-TO-ALGAE RATE, gm CO2 /      2770 R    CO2ALG.K=ALGO2.K*COR
 pond*day; CO2 assimilated
 by algal photosynthesis
AIR/WATER CO2 EXCHANGE RATE      2780 R    AIRCO2.KL=ENF*DCO2*(CO2SAT-CO2.K)
 gm CO2/pond*day                 2785 X              /(DEPTH*ZOX)
CO2 DIFFUSION COEFFICIENT        2790 C    DCO2=1.64
 cm^2/day, Broeker, 1974
```

```
ENHANCEMENT FACTOR                2800 C    ENF=1.0
 values ½ 1 gave unrealisti-
 cally low CO2. See Quinn,
 1971, and Emerson, 1973.
                                  2810 NOTE
                                  2820 NOTE ALKALINITY SECTOR, CaCO3 EQUIVALENTS
                                  2830 NOTE
ALKALINITY, gm CaCO3/pond         2840 L    ALK.K=ALK.J+(DT)(ALK3A.JK+ALK01.JK
 In variable names, 1=ammon-      2850 X    +ALKF1.JK+ALK2N.JK-ALK1A.JK-ALK12.JK
 ia, 2=nitrite, 3=nitrate.        2855 X    +ALKIN.JK)
ALKALINITY, INITIALLY             2860 N    ALK=40*CF
 gm CaCO3/pond; initial alk.
 was 40 mg CaCO3/ liter
ALKALINITY CONCENTRATION          2870 A    ALKCON.K=ALK.K/CF
                                  2880 NOTE
CALCIUM CARBONATE/ NITROGEN       2890 C    CCNR=6.86
 RATIO; molar weight ratio
 of CaCO3 / N
ALK. CHANGE, AMM(1)-TO-ALGAE      2900 R    ALK1A.KL=.5*CCNR*NITAG.K*AMM.K/NTOT.K
 gm CaCO3/pond*day; change
 in alkalinity from ammonia
 assimilation by algae; the
 .5 is from 1 mole of CO3--
 being 2 moles neg. charge;
 see Brewer & Goldman, 1976
ALK. CHANGE, NO3-TO-ALGAE         2910 R    ALK3A.KL=.5*CCNR*NITAG.K*NO3.K/NTOT.K
 gm CaCO3/pond*day; ibid.
ALK. CHANGE, ORG-TO-AMM(1)        2920 R    ALK01.KL=.5*CCNR*OGAM.K
 gm CaCO3/pond*day; change
 from organic decomposition
 and generation of ammonia
ALK. CHANGE, FISH-TO-AMM(1)       2930 R    ALKF1.KL=ALKF1C*CCNR*FSAM.K
 gm CaCO3/pond*day; change        2940 C    ALKF1C=.1
 from fish respiration and
 generation of ammonia
ALK. CHANGE, NO2-TO-NIT.GAS       2950 R    ALK2N.KL=ALK2NC*CCNR*DENIT.K
 gm CaCO3/pond*day; change        2960 R    ALK2NC=.2
 from NO2 denitrification;
 ALK2NC & ALKF1C are lower
 than theoretical .5
ALK. CHANGE, AMM(1)-TO-NO2        2970 R    ALK12.KL=1*CCNR*AMN02.K
 gm CaCO3/pond*day; change
 from ammonia nitrification
 to nitrite. Releases 2 H+,
 thus 1 rather than .5 mult.
ALK. INFLUX, CaCO3 DISSOLU-       2980 R    ALKIN.KL=CACO3D*CLIP(E1.K,E2.K,PH.K,6.35,
 TION, gm CaCO3/pond*day;         2990 C    CACO3D=.08
 Alk. change from dissolving
 CaCO3 from the fish feed.
 If pH ½ 6.35, then use:          3000 A    E1.K=EXP(1.15*(10.33-PH.K))
 If pH ¼ 6.35, then use:          3010 A    E2.K=EXP(2.3*(8.34-PH.K))
                                  3020 NOTE
                                  3030 NOTE PH SECOTR
                                  3040 NOTE
pH (H+ conc. = 10-pH)             3050 A    PH.K=6.35-LCAR.K
LN OF CO2/ALKALINITY RATIO        3060 A    LCAR.K=(LOGN(CO2NZ.K/ALKNZ.K))/2.303
```



```
CARBON DIOXIDE, NONZERO           3070 A    CO2NZ.K=MAX(CO2.K,.01)
 gm CO2/pond; safeguarded
 against nonzero values
 during model development;
 not needed in stnd runs
ALKALINITY, NONZERO (ibid)        3080 A    ALKNZ.K=MAX(ALK.K*.46,.01)
 gm CO2 equivalents /pond
                                  3090 NOTE
                                  3100 NOTE DECOMPOSING (HETEROTROPHIC) BACTERIA (1)
                                  3110 NOTE
DECOMPOSING BACTERIA (BAC1)       3120 L    BAC1.K=BAC1.J+(DT)(BAC1R.JK-BAC1D.JK
 gm N/pond                        3130 X    -BAC1F.JK-BAC10.JK+BAC1S.JK)
DECOMPOSING BACTERIA, INIT.       3140 N    BAC1=BAC1I
 gm N/pond                        3150 C    BAC1I=.1
                                  3160 NOTE
BAC1 REPRODUCTION RATE            3170 R    BAC1R.KL=OGAM.K*BAC1Z
 gm N/pond*day
BAC1 REPRODUCTION COEF.           3180 C    BAC1Z=.05
 gm N bacterial growth per
 gm N organics decomposed
BAC1 DEATH RATE, gmN/pnd*day      3190 R    BAC1D.KL=BAC1.K*BAC1DC
BAC1 DEATH COEF., per day         3200 C    BAC1DC=.02
BAC1 FISH PREDATION RATE          3210 R    BAC1F.KL=BAC1FD.K
 gm N/pond*day                    3220 A    BAC1FD.K=BAC1.K*BACFC*TOXSF.K
                                  3225 X              *FRESP.K/FRI.K
BAC. FISH PRED. COEF., day-1      3230 C    BACFC=.02
BAC1 OUTFLOW RATE, gmN/p*day      3240 R    BAC10.KL=BAC1.K*OOF.K+BAC1.K*FILT
BAC1 SEEDING RATE, gmN/p*day      3250 R    BAC1S.KL=.0025
                                  3260 NOTE
                                  3270 NOTE AMMONIA-OXIDIZING, NITRITE-FORMING
                                  3280 NOTE (NITROSOMONAS) BACTERIA (2)
                                  3285 NOTE
AMMONIA-OXIDIZING BACTERIA        3290 L    BAC2.K=BAC2.J+(DT)(BAC2R.JK-BAC2D.JK
 gm N/pond                        3300 X    -BAC2F.JK-BAC20.JK+BAC2S.JK)
DECOMPOSING BACTERIA, INIT.       3310 N    BAC2=BAC2I
 gm N/pond                        3320 C    BAC2I=.02
                                  3330 NOTE
BAC2 REPRODUCTION RATE            3340 R    BAC2R.KL=AMNO2.K*BAC2Z
 gm N/pond*day
BAC2 REPRODUCTION COEF.           3350 C    BAC2Z=.05
 gm N bacterial growth per
 gm N ammonia oxidized
BAC2 DEATH RATE, gmN/pnd*day      3360 R    BAC2D.KL=BAC2.K*BAC2DC
BAC2 DEATH COEF., per day         3370 C    BAC2DC=.02
BAC2 FISH PREDATION RATE          3380 R    BAC2F.KL=BAC2FD.K
 gm N/pond*day                    3390 A    BAC2FD.K=BAC2.K*BACFC*TOXSF.K
                                  3395 X              *FRESP.K/FRI.K
BAC2 OUTFLOW RATE, gmN/p*day      3400 R    BAC20.KL=BAC2.K*OOF.K+BAC2.K*FILT
BAC2 SEEDING RATE, gmN/p*day      3410 R    BAC2S.KL=.0005
                                  3420 NOTE
                                  3430 NOTE NITRITE-OXIDIZING, NITRATE-FORMING
                                  3440 NOTE (NITROBACTER) BACTERIA (3)
                                  3445 NOTE
NITRITE-OXIDIZING BACTERIA        3450 L    BAC3.K=BAC3.J+(DT)(BAC3R.JK-BAC3D.JK
 gm N/pond                        3460 X    -BAC3F.JK-BAC30.JK+BAC3S.JK)
```

```
DECOMPOSING BACTERIA, INIT.   3470 N    BAC3=BAC3I
 gm N/pond                    3480 C    BAC3I=.02
                              3490 NOTE
BAC3 REPRODUCTION RATE        3500 R    BAC3R.KL=NIT23.K*BAC3Z
 gm N/pond*day
BAC3 REPRODUCTION COEF.       3510 C    BAC3Z=.025
 gm N bacterial growth per
 gm N nitrite oxidized
BAC3 DEATH RATE, gmN/pnd*day  3520 R    BAC3D.KL=BAC3.K*BAC3DC
BAC3 DEATH COEF., per day     3530 C    BAC3DC=.02
BAC3 FISH PREDATION RATE      3540 R    BAC3F.KL=BAC3FD.K
 gm N/pond*day                3550 A    BAC3FD.K=BAC3.K*BACFC*TOXSF.K
                              3555 X              *FRESP.K/FRI.K
BAC3 OUTFLOW RATE, gmN/p*day  3560 R    BAC3O.KL=BAC3.K*OOF.K+BAC3.K*FILT
BAC3 SEEDING RATE, gmN/p*day  3570 R    BAC3S.KL=.0005
                              3580 NOTE
                              3590 NOTE NITRATE-REDUCING, NITRITE-FORMING
                              3600 NOTE DENITRIFYING BACTERIA (4)
                              3605 NOTE
NITRATE-REDUCING BACTERIA     3610 L    BAC4.K=BAC4.J+(DT)(BAC4R.JK-BAC4D.JK
 gm N/pond                    3620 X    -BAC4F.JK-BAC4O.JK+BAC4S.JK)
DECOMPOSING BACTERIA, INIT.   3630 N    BAC4=BAC4I
 gm N/pond                    3640 C    BAC4I=.02
                              3650 NOTE
BAC4 REPRODUCTION RATE        3660 R    BAC4R.KL=NIT32.K*BAC4Z
 gm N/pond*day
BAC4 REPRODUCTION COEF.       3670 C    BAC4Z=.05
 gm N bacterial growth per
 gm N nitrate reduced
BAC4 DEATH RATE, gmN/pnd*day  3680 R    BAC4D.KL=BAC4.K*BAC4DC
BAC4 DEATH COEF., per day     3690 C    BAC4DC=.02
BAC4 FISH PREDATION RATE      3700 R    BAC4F.KL=BAC4FD.K
 gm N/pond*day                3710 A    BAC4FD.K=BAC4.K*BACFC*TOXSF.K
                              3715 X              *FRESP.K/FRI.K
BAC4 OUTFLOW RATE, gmN/p*day  3720 R    BAC4O.KL=BAC4.K*OOF.K+BAC4.K*FILT
BAC4 SEEDING RATE, gmN/p*day  3730 R    BAC4S.KL=.0005
                              3740 NOTE
                              3750 NOTE NITRITE-REDUCING, N2 GAS-FORMING
                              3760 NOTE DENITRIFYING BACTERIA (5)
                              3765 NOTE
NITRITE-REDUCING BACTERIA     3770 L    BAC5.K=BAC5.J+(DT)(BAC5R.JK-BAC5D.JK
 gm N/pond                    3780 X    -BAC5F.JK-BAC5O.JK+BAC5S.JK)
DECOMPOSING BACTERIA, INIT.   3790 N    BAC5=BAC5I
 gm N/pond                    3800 C    BAC5I=.02
                              3810 NOTE
BAC5 REPRODUCTION RATE        3820 R    BAC5R.KL=DENIT.K*BAC5Z
 gm N/pond*day
BAC5 REPRODUCTION COEF.       3830 C    BAC5Z=.10
 gm N bacterial growth per
 gm N nitrite reduced
BAC5 DEATH RATE, gmN/pnd*day  3840 R    BAC5D.KL=BAC5.K*BAC5DC
BAC5 DEATH COEF., per day     3850 C    BAC5DC=.02
BAC5 FISH PREDATION RATE      3860 R    BAC5F.KL=BAC5FD.K
 gm N/pond*day                3870 A    BAC5FD.K=BAC5.K*BACFC*TOXSF.K
                              3875 X              *FRESP.K/FRI.K
BAC5 OUTFLOW RATE, gmN/p*day  3880 R    BAC5O.KL=BAC5.K*OOF.K+BAC5.K*FILT
```



```
BAC5 SEEDING RATE, gmN/p*day  3890 R    BAC5S.KL=.0005
                              3900 NOTE
                              3910 NOTE ACTUAL MEASURED DATA
                              3920 NOTE
FISH BIOMASS, gm wet wt.      3930 A    FIX.K=TABHL(FIXT,TIME.K,0,98,14)
                              3940 T    FIXT=2000/3400/3900/4500
                              3945 X        /5000/5000/6000/7000
TOXICITY (weighted index)     3950 A    TOX.K=TABHL(TOXT,TIME.K,0,98,7)
                              3960 T    TOXT=0/1.5/3/2.5/2/4/4/5
                              3965 X        /5/6/4/1.5/.5/1.5/2.5
OXYGEN, mg/liter              3970 A    OXX.K=TABHL(OXXT,TIME.K,0,98,7)
 av. midday measurements      3980 T    OXXT=9.4/11.1/11.4/11.6/13.7/11.5/7.8/7.7
                              3990 X        /5.6/1.7/5.3/8.6/7.2/13.3/11.9
AMMONIA, mg N/liter           4000 A    AMX.K=TABHL(AMXT,TIME.K,0,98,7)
 av. midday measurements      4010 T    AMXT=0/3/9/7/3/3/1/1/10/15/11/1/1/1/2
TOTAL NITROGEN, mg N/liter    4020 A    NTOTX.K=TABHL(NTOTXT,TIME.K,0,98,7)
 av. midday measurements      4030 T    NTOTXT=0/3/10/7/3/7/10/7
                              4035 X          /14/15/14/6/9/29/12
NITRITE, mg N/liter           4040 A    NO2X.K=TABHL(NO2XT,TIME.K,0,98,7)
 av. midday measurements      4050 T    NO2XT=0/0/0/0/0/2/2/2/2/0/2/2/5/10/10
NITRATE, mg N/liter           4060 A    NO3X.K=NTOT.K-AMX.K
pH                            4070 A    PHX.K=TABHL(PHXT,TIME.K,0,98,7)
 av. midday measurements      4080 T    PHXT=8.3/8.2/7.3/7.7/8.6/7.1/6.4/6.3/6.7
                              4090 X        /7.0/6.7/6.1/6.0/5.9/5.5
ALKALINITY, mg CaCO3/liter    4100 A    ALKX.K=TABHL(ALKXT,TIME.K,0,98,7)
 av. midday measurements      4110 T    ALKXT=40/42.5/46.7/40/40/42.5/40/37.5
                              4120 X          /61.7/68.5/60/13.8/15/12.5/10
TEMPERATURE, Celsius          4130 A    TEMP.K=TABHL(TEMPT,TIME.K,0,98,7)
 av. midday measurements      4140 T    TEMPT=24.7/25.9/29.2/28.2/24.8/26.2/22.3
                              4150 X    /26.1/29.9/29.9/25.1/25.9/26.4/26.1/23.2
FIRST ACIDITY pK              4160 A    TK1.K=TABHL(TK1T,TEMP.K,5,30,5)
                              4170 T    TK1T=6.52/6.47/6.42/6.38/6.35/6.33
SECOND ACIDITY pK             4180 A    TK2.K=TABHL(TK2T,TEMP.K,5,30,5)
                              4190 T    TK2T=10.55/10.45/10.43/10.38/10.33/10.29
USED TO CALCULATE CO2 FROM    4200 A    BASE1.K=1+2*EXP(-TK2.K*LOGN(10))
 pH AND ALKALINITY            4205 X              /EXP(-PHX.K*LOGN(10))
                              4210 A    BASE2.K=BASE1.K*EXP(-TK1.K*LOGN(10))
CARBON DIOXIDE, mg CO2/liter  4220 A    CO2X.K=.44*ALKX.K*EXP(-PHX.K*LOGN(10))
                              4225 X          /BASE2.K
ALGAE BIOVOLUME               4230 A    ALGX.K=TABHL(ALGXT,TIME.K,0,98,7)
 10^7 microns^3/milliliter    4240 T    ALGXT=2/5/4/1/12/48/18/12/4/1/8/5/3/10/14
ALGAE, gm N/2300 liter pond   4250 A    AX.K=ALGX.K*AXC
ALGAE CONVERSION COEFFICIENT  4260 C    AXC=.31
 based on dry/wet ratio of
 .15 & N/dry ratio of .09
                              4270 NOTE
                              4280 NOTE NITROGEN TRACKING VARIABLES, GM N/POND
                              4290 NOTE "STACKS" VARIABLES ON TOP OF EACHOTHER
                              4300 NOTE
NITROGEN FEED INPUT,          4310 A    NFED.K=FED.K+FEDNC
 CUMULATIVE
NITROGEN IN FISH BIOMASS      4320 A    NFIS.K=FISH.K*FISNC
NITROGEN IN ORGANICS          4330 A    NORG.K=NFIS.K+ORG.K
NITROGEN IN ALGAE             4340 A    NALG.K=NORG.K+ALG.K
NITROGEN AS SOLUBLE INOR-     4350 A    NAMM.K=NALG.K+AMM.K+NO2.K+NO3.K
 GANIC COMPOUNDS: AMMONIA,
 NITRITE AND NITRATE
```

```
NITROGEN ESCAPING AS AMMONIA 4360 L    INH3.K=INH3.J+(DT)(NH3AIR.JK)
                             4370 N    INH3=0
                             4380 A    NNH3.K=NAMM.K+INH3.K
NITROGEN ESCAPING AS N2 GAS  4390 L    IN2.K=IN2.J+(DT)(NO2N2.JK)
                             4400 N    IN2=0
                             4410 A    NN2.K=IN2.K+NNH3.K
NITROGEN REMOVED IN DRAIN-   4420 L    IOUT.K=IOUT.J+(DT)(AMMOUT.JK+ALGOUT.JK
 DOWNS                       4430 X          +ORGOUT.JK+NO2OUT.JK+NO3OUT.JK)
                             4440 N    IOUT=0
                             4450 A    NOUT.K=IOUT.K+NN2.K
CUMULATIVE NITROGEN INPUT:   4460 A    NIN.K=NFED.K+FISHI*FISNC+ALGI
 initial fish and algae
 plus feed input
                             4470 NOTE
                             4480 NOTE
                             4490 NOTE SPECIFICATIONS
                             4500 NOTE
SIMULATION & OUTPUT SPECS    4510 SPEC LENGTH=98/DT=.05/PLTPER=2/PRTPER=0
 Run Length = 98 days
 Time Increment, dt = .05 day
 Plot Increment = 2 days
 Print Inc.= 0 (no printing)
 Mark @ 14 days (7 PLTPERs)  4520 DTSS LINE=7
PLOT nitrate as "3" on the   4530 PLOT NO3CON=3,NO2CON=2,AMMCON=1/OXCON=0(0,*)/
 same unit scale (mg N/ltr)  4540 X    ASSIM=%(0,.32)/ORG=S(0,*)/ALG=A(0,*)/
 as NO2 and ammonia; etc.    4545 X    FISH=F(2000,*)
PRINT VALUES                 4550 PRINT FISH,FED,FCRA,GROWTH,GRORAT
```

****

** Variables where units are not explicitly stated are dimensionless, i.e., they are fractions, dimensionless coefficients, or relative indices referenced to zero, one, or a specific range.

*** Table functions are a convenient way of expressing nonlinear relationships in DYNAMO. TABHL(ASSFT,TOXIN.K,0,10,1) means that the ASSIMILATION FACTOR is a function of the TOXICITY INDEX in the range of 0 to 10 units, specified in steps of 1 unit. ASSFT=1.0/.92/.9/.8/.6/.4/.3/.2/.1/.05/.02 "draws" a piece-wise linear S-curve where ASSFT has a value of 1 at a TOXICITY INDEX of 0, .92 at TOXIN of 1, .2 at 7 and .02 at 10.

**** Some DYNAMO compilers, including the one used here, constrain .KL rates so that they cannot be a function of other .KL rates. Under this constraint, the algae growth rate, NITALG.KL, cannot directly determine the rate of oxygen generated by algae, ALGOX.KL. To circumvent this compiler limitation, several

***** A Z-film thickness is an idealized air/liquid boundary layer gap across which a gas evenly diffuses at a rate determined by molecular diffusion. The z-film is greatly influenced by aeration and surface agitation. The following table displays the range of z-films possible. It is derived from experiments using abiotic solar-algae ponds purged of oxygen and then monitored for reoxygenation (NSF Progress Report 2, p.14). The table was constructed noting that:

Z-FILM THICKNESS = OXYGEN DIFFUSION COEF/(REOX TIME COEF * POND DEPTH)

CONDITION	REOXYGENATION TIME COEFFICIENT per hr	per day	Z-FILM THICKNESS cm
still air	0.007	00.17	.08
wind	0.025	00.60	.023
weak aeration	0.120	02.90	.005
strong aeration	1.600	38.00	.00036

Because atmospheric ammonia is so slight, NH_3 always tends to diffuse from the pond. Because un-ionized ammonia only occurred in significant concentrations during high pH daytime periods when the aeration was switched off, the z-film thickness for ammonia, ZAM, reflects nonaeration conditions. For oxygen, however, the greatest difference between equilibrium and actual pond concentrations occurred at night, when oxygen levels are lowest. Thus ZOX reflects nighttime aeration conditions.

****

TRANSLATION FROM DYNAMO EQUATIONS TO STANDARD CALCULUS NOTATION:

In DYNAMO, the numeric integration by the model is indicated in the L (level, or state variable) equations:

L FISH.K=FISH.J+(DT)(FISHGRO.JK)

which is algebraically computed in the model: $fish_t = fish_{t-dt} + dt*fishgro_{t-dt}$

Variables are initialized: N FISH=2010, i.e., $fish_{t=0} = 2010$ (grams)

The extensions .J, .K, .L, .JK and .KL on DYNAMO variables indicate points in the time simulation:

.J = t - dt
.K = t
.L = t + dt
.JK = from (t - dt) to (t)
.JL = from (t) to (t + dt)